Tribological Evaluation of Various Aluminum Alloys in Lubricant/Refrigerant Mixtures

T. K. Sheiretov, H. Yoon and C. Cusano

ACRC TR-92 January 1996

For additional information:

Air Conditioning and Refrigeration Center
University of Illinois
Mechanical & Industrial Engineering Dept.
1206 West Green Street
Urbana, IL 61801

(217) 333-3115

Prepared as part of ACRC Project 49
Compressor—Lubrication, Friction and Wear
C. Cusano, Principal Investigator

The Air Conditioning and Refrigeration Center was founded in 1988 with a grant from the estate of Richard W. Kritzer, the founder of Peerless of America Inc. A State of Illinois Technology Challenge Grant helped build the laboratory facilities. The ACRC receives continuing support from the Richard W. Kritzer Endowment and the National Science Foundation. The following organizations have also become sponsors of the Center.

Amana Refrigeration, Inc.
Brazeway, Inc.
Carrier Corporation
Caterpillar, Inc.
Dayton Thermal Products
Delphi Harrison Thermal Systems
Eaton Corporation
Electric Power Research Institute
Ford Motor Company
Frigidaire Company
General Electric Company
Lennox International, Inc.
Modine Manufacturing Co.
Peerless of America, Inc.
U. S. Army CERL
U. S. Environmental Protection Agency
Whirlpool Corporation

For additional information:

Air Conditioning & Refrigeration Center
Mechanical & Industrial Engineering Dept.
University of Illinois
1206 West Green Street
Urbana IL 61801

217 333 3115

TRIBOLOGICAL EVALUATION OF VARIOUS ALUMINUM ALLOYS IN LUBRICANT/REFRIGERANT MIXTURES

ABSTRACT

The tribological characteristics of various aluminum alloys, aluminum composites and some surface treated aluminum are evaluated in lubricant/refrigerant mixtures. All of these evaluations are based upon a specimen testing program using a high pressure tribometer (HPT). This research program mainly consists of two parts.

The first part of this study is mainly focused on materials screening of various aluminum alloys/steel contact pairs lubricated by polyolester/R134a and PAG/R134a lubricant/refrigerant (L/R) mixtures. In this study, various aluminum alloys are tested under the same environmental and operating conditions in order to compare their wear resistance. The results show that the lowest wear is obtained with the 390 Die Cast alloy. This alloy has the largest amount of silicon content and the highest bulk hardness. The results also show that, in general, the amount of wear decreases as the amount of silicon content in Al-Si alloys increases. Better wear resistance is also achieved if the amount of copper and bismuth are increased. Conventional anodizing does not improve the wear resistance of the 356 aluminum alloy under concentrated contacts. Hard anodizing and a SiC-Al composite provide very good wear resistance. However, they cause increased wear on the counterface by abrasion due to the rough, hard, surfaces generated by hard anodizing processes and the hard SiC particles. From the wear results obtained, the Ester/R134a mixtures consistently provide better protection of the aluminum alloys compared to the PAG/R134a mixtures. If sufficient amounts of R134a exists in the L/R mixture, extensive surface fatigue on 356 aluminum is observed.

In the second part, two Al-Si alloys (356-T61 and 390-T61), widely used in critical components of refrigerant compressors, are examined for their friction and wear behavior in different L/R mixtures. The L/R mixtures tested include ester and PAG lubricants with R134a, mineral and alkylbenzene lubricants with R22, R407C and R410A, as well as an ester lubricant with both R407C and R410A. Based on the wear data obtained, the capped PAG seems to be a better lubricant for 356 alloy than the uncapped PAG. However, the lubricity of the PAG's is about the same with the 390 alloy. When the ester lubricant is used, the wear on each alloy is about the same in R134a, R407C, R410A and air environments. There is no significant difference in lubricity of mineral and alkylbenzene lubricants when used with R22 and its possible substitutes R407C and R410A.

1. INTRODUCTION

Various types of aluminum alloys are continually being developed to improve their wear resistance. Among these alloys, aluminum-silicon (Al-Si) alloys have been found to be beneficial in many industrial applications and considered to be appropriate substitutes for cast iron components [1-10]. The addition of silicon in aluminum alloys improves their wear, casting, machining and corrosion characteristics. Both hypoeutectic and hypereutectic Al-Si alloys are widely used in a variety of applications, including automotive [3-8, 10] and related equipment, air-conditioning equipment and home electrical appliances [7, 9, 11].

A large number of studies in recent years have been devoted to investigate the friction and wear behavior of Al-Si alloys. However, most of these studies were conducted under dry sliding conditions. The few studies that have been conducted under lubricated sliding conditions were mainly concerned with the effect of silicon content and silicon morphology on the friction and wear resistance of these alloys. Also, the friction and wear tests for these studies were conducted mostly in an air environment. Al-Si alloys are widely used for critical components in refrigerant compressors, especially connecting rods in reciprocating compressors and swash plates in automotive air-conditioning compressors. The successful operation of compressors used in air-conditioning and refrigeration systems is mainly governed by the tribological behavior at the critical contacts within the compressors. It is known that the environmental conditions around these contacts have a significant impact on their tribological performance. Thus, the friction and wear characteristics of Al-Si alloys in a refrigerant environment might be quite different from those of Al-Si alloys in an air environment.

In this study, the high pressure tribometer (HPT) is used to evaluate friction and wear characteristics of Al-Si alloys in refrigerants environments. Various types of Al-Si alloys, aluminum composites and some surface treated aluminum alloys are evaluated in various lubricant/refrigerant mixtures. Most of the friction and wear data obtained are for 356-T61 coupon mold and 390-T61 permanent mold aluminum alloys. The effects of the viscosity of the L/R mixture and the initial surface roughness of the aluminum specimens are also evaluated.

2. LITERATURE REVIEW

Due to the importance of aluminum in manufacturing, a large number of studies have been devoted to the investigation of its friction and wear characteristics under various conditions and environments. The published work in this field falls broadly in the following major categories:

1. Effects of metallurgical composition and structure on tribological behaviour.
2. Boundary lubricants for aluminum.
3. Effects of environment on tribological properties of aluminum.

A brief literature review on the wear of aluminum is given in this section. The discussion follows the above classification.

2.1 Effects of Metallurgical Composition and Structure on Tribological Behavior

These studies can be further subdivided depending on the alloying elements studied. Most of the work has been devoted to the effects of silicon, copper, zinc, and lead. In addition, various aluminum composites have been evaluated. The major results from these studies are summarized below:

2.1.1 The Effect of Silicon

Silicon has received the most attention among all alloying elements studied. This is due to the fact that Al-Si alloys are corrosion resistant, strong, have low thermal expansion coefficients, and have superior tribological characteristics compared to the other aluminum alloys [1-10]. These alloys have been successfully used as substitutes for cast iron in applications such as pistons and cylinder linings for internal combustion engines [3-8, 10], swash plates, connecting rods, and sockets in refrigerant compressors [7, 9, 11].

2.1.1.1 Optimal Silicon Content for Wear Resistance

Most researchers [2-4, 6, 12, 13] agree that the wear rate of Al-Si alloys goes through a minimum at certain Si content. The higher wear rates at low Si contents are attributed to the lower hardness of these alloys, while the increased wear rates at high Si contents are due to reductions in their ductility and fracture toughness. Although there is some controversy in the literature about the location of this minimum, it seems that for weaker and more brittle binary Al-Si alloys, the minimal wear rate is achieved with alloys having Si content at or slightly higher than the eutectic composition (12.6%) [2-4, 6, 14]. For the commercial alloys which have other alloying elements to improve their strength and toughness (e.g. Cu and Mg), the minimum is usually shifted to higher Si contents (e.g. 17%) [12, 13]. Probably the most popular commercial alloy with 17% Si is the 390 alloy which is used in numerous applications where high wear resistance is required [9].

2.1.1.2 Wear Regimes

It is generally accepted [2, 4, 5, 7, 10, 12, 14-17] that there are two distinct wear regimes for the Al-Si alloys. The difference in the wear rates of these regimes can be as high as two orders of magnitude [2, 5]. The mild wear regime is characterized by the formation of small (< 5 μm) [5, 8, 15, 19] equiaxed wear particles. These wear particles are usually black in color [5, 8, 17] and are comprised primarily of aluminum oxide. Hence, in mild wear regime, an oxidative wear mechanism is assumed to dominate [5, 12, 17].

The severe wear regime is characterized by the formation of larger wear particles (> 15 μm), some of which are metallic [8, 19]. These wear particles are assumed to be formed by a surface fatigue (delamination) process. There is a controversy about the conditions at which the transition from mild to severe wear occurs. Most transitions in dry condition seem to occur at contact pressures (for an area contact) of 0.8 to 2.0 MPa [5, 18], but values as low as 0.2 MPa [14], or as high as 22 MPa [2] have also been reported. The transition load also changes with the sliding velocity, being higher at the higher velocities. The explanation for this behavior is that the higher temperatures generated at the higher sliding velocities favor the oxidative wear mechanism [12].

2.1.1.3 Optimal Size of the Silicon Particles

There is also a controversy about the optimal size of the silicon particles. The results differ depending on the conditions of the tests conducted. Researchers, who have conducted tests under dry conditions, tend to agree that the initial size of Si particles is not important [2, 3, 5, 12, 19, 20]. Under dry conditions, the rubbing surfaces are subjected to severe traction which often causes plastic flow of the subsurface layer. Under these conditions, the silicon particles fracture and attain some equilibrium size (1-5 μm) and shape (spherical), irrespective of their initial size and shape [2, 14, 21]. The strain hardening of the subsurface, together with some compaction of wear debris, form a work-hardened layer which is characterized by much higher hardness (240 HV compared to 100 HV of the bulk alloy) [4, 12]. This layer protects the surface from further damage.

If the sliding occurs under lubricated conditions, a work-hardened layer usually is not formed [9, 10] and the microstructure remains unchanged up to the surface. Under these conditions, the size and shape of the silicon particles becomes important. Larger silicon particles are more effective in modifying the counterface by removing the preferred sites for aluminum transfer and in polishing away of any adhered aluminum [22, 23]. On the other hand, larger Si particles cause higher temperature spikes which may lead to thermally driven seizure [23]. Alloys with finer silicon particles also have higher hardnesses [12], which is an important parameter for better wear resistance.

2.1.2 The Effect of Copper

Copper increases the strength and wear resistance of aluminum alloys through a mechanism of precipitation hardening. The wear and seizure resistance of Al-Cu alloys were found to increase up to Cu contents of about 4%, after which it levels off [24]. The highest wear resistance is obtained with the peak aged precipitates [16].

2.1.3 The Effect of Lead

Lead containing aluminum alloys are used for journal bearings. The friction and wear of alloys containing up to 50% lead have been studied [18, 25, 26]. The optimum performance was achieved with a lead content of 25%. Higher Pb contents decrease the strengths of the alloy, and bring about higher wear. These alloys are also less seizure resistant because the subsurface layers tend to flow plastically at lower loads [26]. If the Pb content is low, the alloy is not able to form a smeared lead layer at the interface and is, therefore, more prone to seizure and higher wear [26]. Aluminum-lead alloys, however, are hard to manufacture due to the immiscibility of Al and Pb even in the molten state. Special casting techniques are required [26].

2.1.4 The Effects of Other Chemical Elements

Zinc reduces both wear resistance and seizure resistance of aluminum alloys [24]. The reason is the reduced strength of the alloys at elevated interfacial temperatures.

The addition of magnesium up to 1% is also useful in reducing wear. It is added to provide strengthening through precipitation of Mg_2Si in the matrix [1]. However, large amounts of magnesium degrade the mechanical properties of aluminum alloys [1, 16].

Iron is the most common alloying element for aluminum. It can be tolerated up to levels of 1.5-2.0% [1]. The presence of iron modifies the silicon phase by introducing several Al-Fe-Si phases. If present alone, iron forms intermetallic compound with aluminum at grain boundaries and impairs mechanical properties [16]. When elements such as manganese, chromium, cobalt and molybdenum are present, iron combines with them to form intermetallic compounds which are less harmful.

Other elements usually added to aluminum include nickel, titanium and zirconium (grain refiners), sodium and strontium (eutectic silicon modifiers) and phosphorus (primary silicon refiner) [1, 16].

2.1.5 Aluminum Matrix Composites

Aluminum-matrix particle composites represent some of the lowest cost composites. They are also among the most widely used in tribological applications [27]. Some of these composites can be manufactured by a conventional die casting or squeeze casting process [27, 28]. The aluminum matrix composites can be classified in two groups: those containing hard particles (SiC, Al_2O_3, silica) and those

containing soft particles (graphite, MoS_2). Of all the aluminum-base composites, the composites containing graphite have the lowest wear [27, 29].

The ultimate tensile strength of Al composites increases with the volume fraction of hard particles and decreases with the volume fraction of soft particles. The wear resistance and the fracture toughness, however, tend to increase with increasing volume fraction of both hard and soft particles [27-29]. Adhesive or abrasive wear rate is inversely proportional to the particle size in composites containing either hard or soft particles [27].

2.2 Boundary Lubricants for Aluminum

Under boundary lubrication conditions, the ability of the lubricant to form protective boundary films is very important. Due to the differences in the chemical properties of aluminum and iron, most of the boundary lubricants designed for ferrous materials fail to form protective films on aluminum [30, 31]. A large variety of organic compounds including adipic esters [31], alcohols and ethers [32], polyglycols [33], phthalic esters [34], manolic diesters [35, 36] have been systematically studied. Among these, the adipic esters and the oxygen containing substances which are able to form bidentate bonds with aluminum were the most effective [31, 35, 36] as boundary lubricants for aluminum. Polyolester synthetic lubricants are among the best boundary lubricants for aluminum due to their ability to form bidentate bonds with the Al surface. It seems that there are two general requirements to effectively boundary lubricate aluminum: (a) the lubricant should be able to form protective films on a bare aluminum surface (a double carbon bond [37] or carbon-oxygen bond [36] should be present in the lubricant molecule) and (b) the lubricant should be able to form a protective film on aluminum oxide (a polar group is necessary [37]). With effective boundary lubrication, the wear is primarily chemical and the alloy microstructure remains intact up to the surface [31].

2.3 Effects of Environment on Tribological Properties of Aluminum

The environment affects the tribological properties of aluminum alloys by (a) chemical reactions of active species with aluminum and (b) by changes in the oxidizing ability of the environment. Therefore, the friction and wear results obtained under inert environments could be different from those obtained in an air environment.

The properties of the aluminum oxide present on the surface often determine the tribological behavior of aluminum, especially under dry sliding conditions. Stronger oxides are considered to be beneficial [38]. Oxides produced by anodic treatment are dense and are under compressive residual stresses. They can withstand higher loads without rupturing, providing better wear and seizure resistance [38]. Water was also found to have a beneficial effect on friction and wear under an air

environment [6, 39]. It is believed that water reacts with Al_2O_3 to form aluminum hydroxides which have layered structure and may act as solid lubricants [39].

Changes in the tribological behavior of aluminum alloys also occur when the contact pair operates under refrigerant environments [11, 39-41]. The CFC refrigerants are known to form chlorides with the metal surfaces which act as boundary lubricants [40, 41]. The HFC's can also react with aluminum to form fluorides [10]. The tribological properties of aluminum fluorides are less studied. There are, however, some indications that their effect, if any, is detrimental [11]. The formation of oxides is significantly impaired under refrigerant environments. The oxides have positive effects, provided that the lubricant forms effective protective films on bare metal aluminum [39].

3. DESCRIPTION OF THE EXPERIMENTS

3.1 Apparatus

All tests in this study were conducted in the High Pressure Tribometer (HPT) which provides accurate control of both test environment and operating conditions. For this experimental program, two new measuring systems were installed in the HPT: (a) an in-line viscometer, and (b) an electric contact resistance measuring circuit. A schematic of the HPT's pressure chamber and the viscometer is shown in Fig. 1.

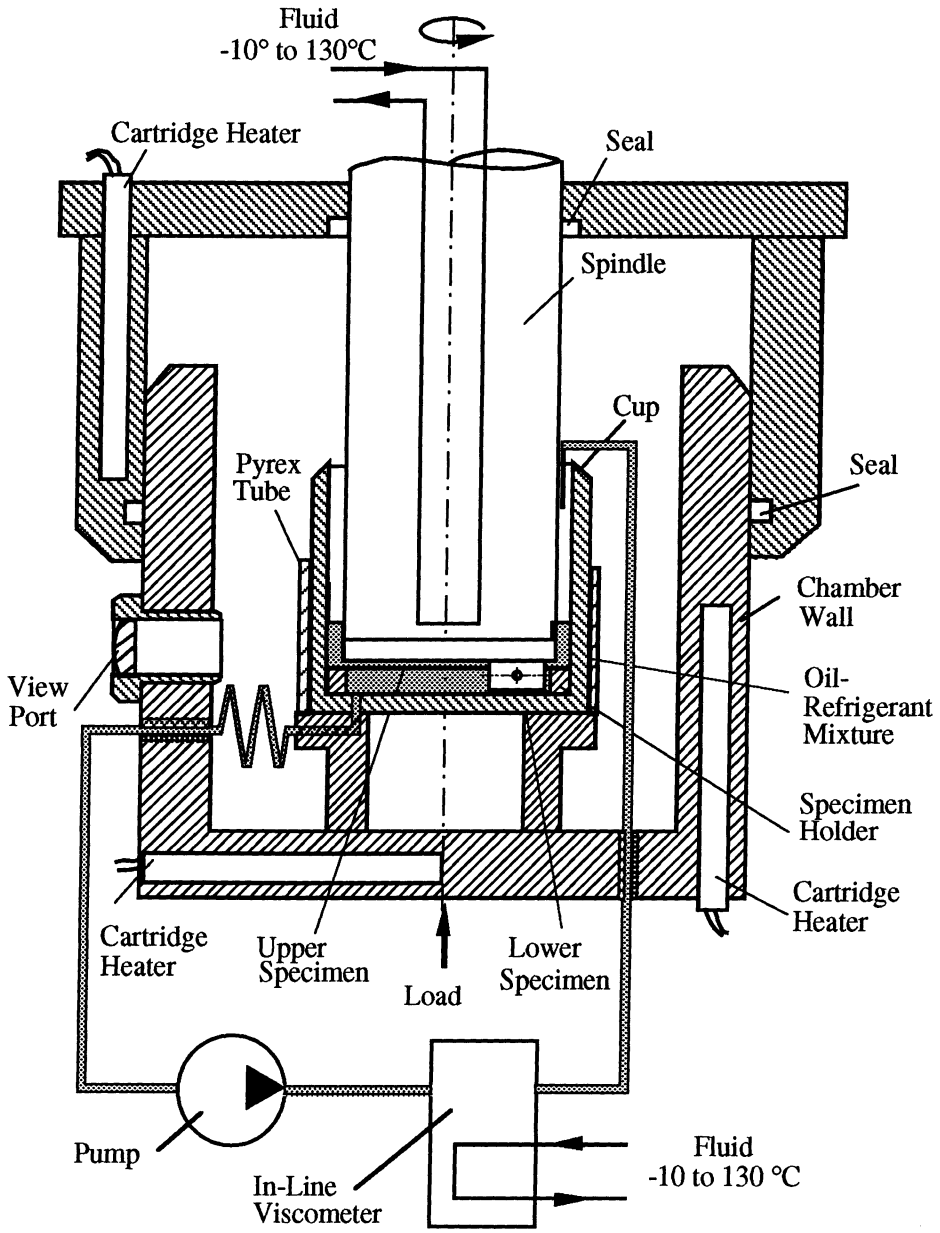

Fig. 1 - Schematic of the HPT's Pressure Chamber with an In-Line Viscometer

The in-line viscometer provides in-situ information about the viscosity changes of the L/R mixture. The viscosity of the mixture was measured by circulating the pressurized mixture through the viscometer. Changes in the viscosity of the lubricant/refrigerant mixtures were monitored inside the pressure chamber of the HPT for one hour.

The contact resistance measuring circuit provides indirect information about the regime of lubrication, the formation of protective surface films, the extent of metal-to-metal contact and the material transfer. A schematic of the circuit is given in Fig. 2.

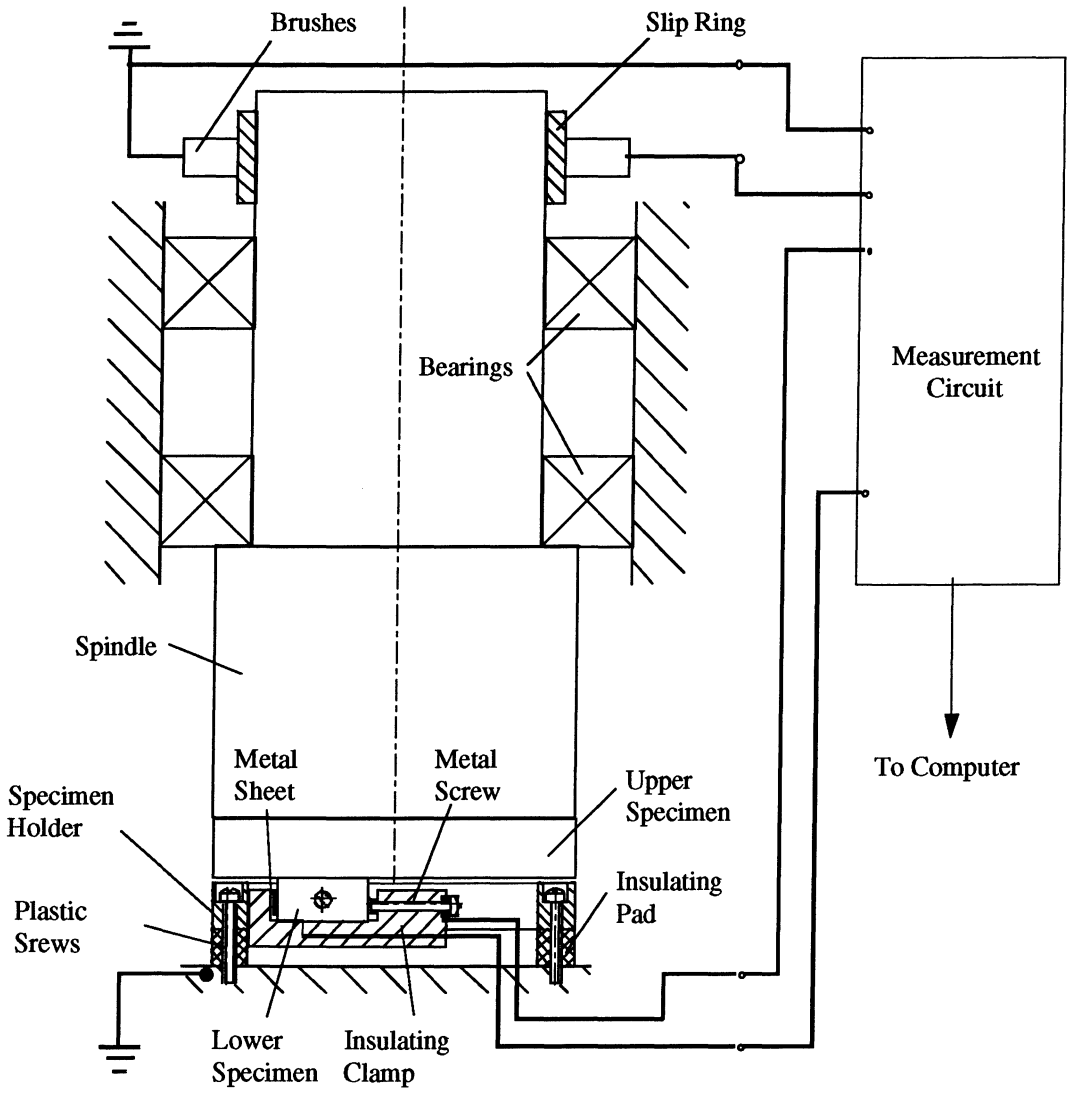

Fig. 2 - A Schematic of the Contact Resistance Measuring Circuit

The measuring circuit utilizes the four-terminal measuring method which enables the measurement of electric resistance in the range of 10^{-6}-10^{4} Ω. The circuit is controlled by a computer which provides an automatic adjustment of the amplifier gains, depending on the measuring range and compensation for any thermal effects that can be caused by frictional heating. Typical records showing

the changes of the contact resistance and the coefficient of friction during the test are given in Fig. 3. Note that low values of the contact resistance correspond to spikes of the coefficient of friction.

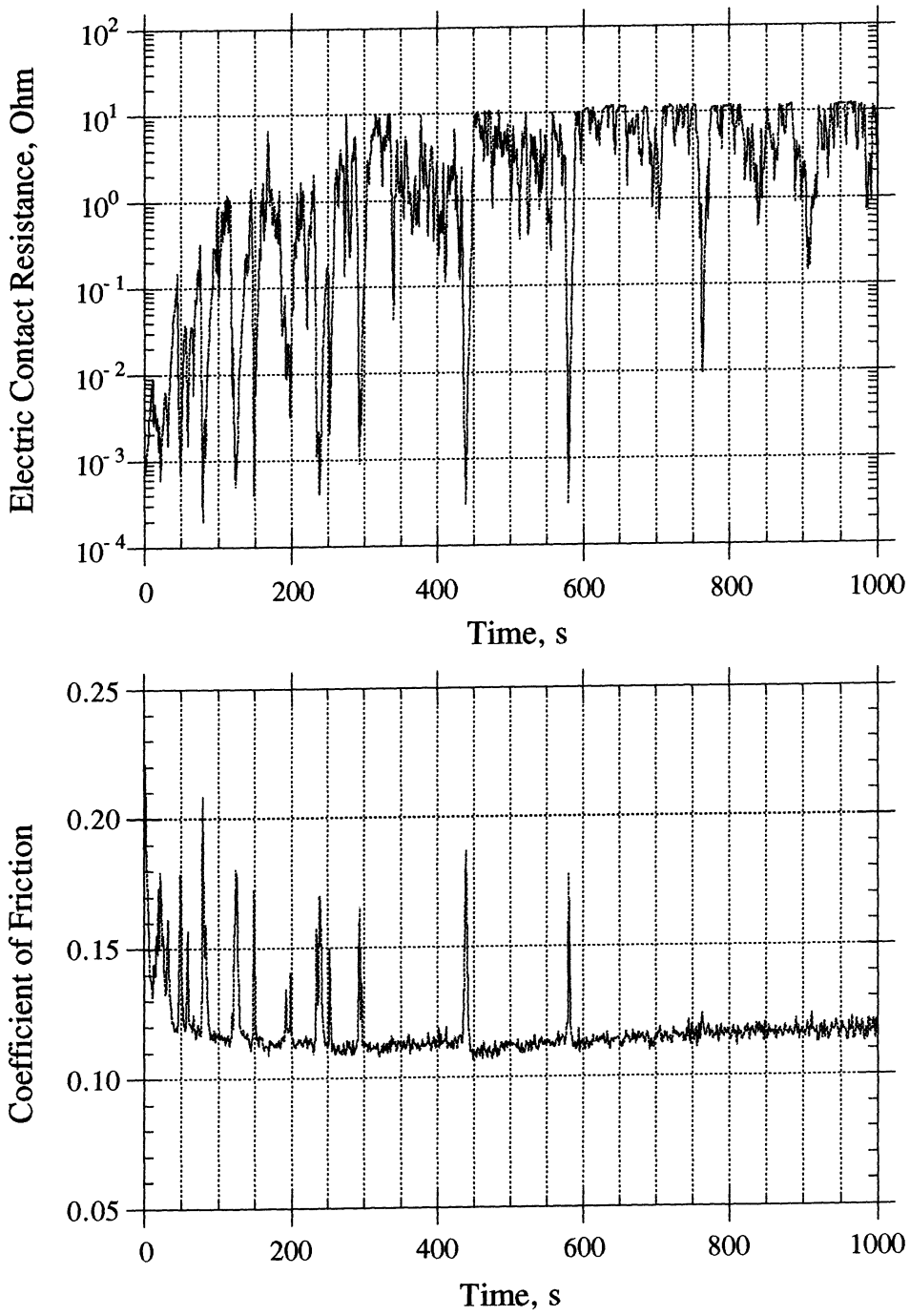

Fig. 3 - Records of the Electric Contact Resistance and the Coefficient of Friction for the First 1000 s of a Test Conducted Under Condition C (Table 3) Aluminum Alloy Tested: 356CM-T61 (Table 1), Amount of Material Transfer: Large

3.2 Geometry of Contact

Concentrated line contact was used for this set of experiments. A cylindrical pin having a diameter of 6.35 mm (0.25 in.) and a length of 6.35 mm (0.25 in.) was slid over an aluminum alloy disc. The wear track on the disc is a circular area with an average radius of 10 mm (0.384 in.). A representation of the contact geometry is given in Fig. 4. The lower specimen is secured in place by a specimen holder and the upper specimen is attached to the rotating spindle.

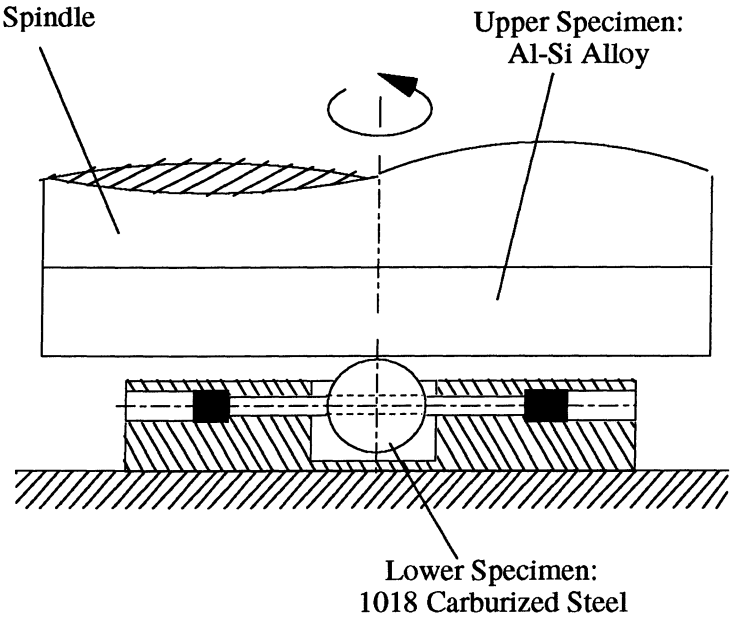

Fig. 4 - Geometry of Contact

3.3 Materials for the Test Specimens

An outline of the major set of tests conducted is given in Table 1. The numbers under "test conditions" represent the number of times the tests were reproduced. One widely used ester (condition A) and PAG (condition C) were chosen for the materials screening tests in R134a environment. The rows for 390PM-T61 and 356CM-T61 represent testing of these aluminum alloys under various conditions. Information about the various alloys tested, the heat or surface treatment, the method of fabrication, and the surface hardness is also provided in Table 1. The HV3-T4, HV3-T6, HV4-T61 and C278-T4 aluminum alloys were provided by Harrison, a division of GM, and the same designations are used in Table 1. The chemical compositions of the C278 and 4032 alloys are very similar, except for the presence of small amounts of Bi and Pb. The chemical composition of the aluminum alloys tested is given in Table 2. For all tests conducted, the pin material was 1018 carburized steel with a surface hardness of 773±78 HV and a surface roughness of 0.25±0.06 μm Ra.

Table 1 - Material Designation and Tests Conducted

Material Designation	Treatment	Fabrication	Hardness HRB	Test Conditions Designated in Table 3																
				A	B	C	D	E	F	G	H	I	J	K	L	M	N	O	P	Q	R
HV3-T6	T6	Extrusion	46	2		2															
HV3-T4	T4	Extrusion	44	2		2															
HV4-T61	T61	Squeeze Cast	51	2		2															
C278-T4	T4	Extrusion	47	2		2															
6061-T61	T61	Extrusion	48	2		2															
2024-T351	T351	Extrusion	58	2		2															
390DC-T6	T6	Die Cast	74	2		2															
390PM-T61	T61	Permanent Mold	56	3	2	2	2	2	2	2	2	3	2		2	2	2	2	2	2	4
356DC-NT	Not Treated	Die Cast	46	2		2															
356PM-T61	T61	Permanent Mold	46	2		2															
356CM-T61	T61	Coupon Mold	49	3	2	3	2	2	2	2	2	3	2	2	2	2	2	2	2	2	3
356CM-NT	Not Treated	Coupon Mold	38	2		3															
356CM-AN	Anodizing	Coupon Mold	49	2		2															
356CM-HC	‡ Hardcoat®	Coupon Mold	600 HV											2							
356CM-NF	‡ Nituff®	Coupon Mold	600 HV											2							
SiC-Al		Die Cast	41											2							
‡ Hardcoat® and Nituff® are proprietary hard anodizing processes																					

Table 2 - Chemical Composition of the Aluminum Alloys Tested

Alloy	Alloying Elements, % by Weight										
	Si	Fe	Cu	Mn	Mg	Cr	Ni	Zn	Bi	Pb	Ti
356	6.5-7.5	0.6	0.25	0.35	0.25-0.45	-	-	0.35	-	-	0.25
390	16-18.5	1.0	3.0-4.0	0.5	0.4-1.0	-	-	1.0	-	-	0.25
HV3	6.5-12	0.20	2.0-5.0	0.15	-	-	-	0.15	1.0-5.0	-	0.20
HV4	11-13.5	1.0	2.0-5.0	0.50	-	-	1.5-2.5	0.15	3.0-6.0	-	0.20
C278	11-13.5	1.0	0.5-1.3	-	0.8-1.3	0.10	0.5-1.3	0.25	0.50	0.50	-
2024	0.50	0.50	3.8-4.9	0.3-0.9	1.2-1.8	0.10	-	0.25	-	-	0.15
6061	0.4-0.83	0.70	0.15-0.4	0.15	0.8-1.2	0.04-0.35	-	0.25	-	-	0.15

SEM pictures of the microstructure of four 356 alloys with different method of fabrication or surface treatment are shown in Fig. 5. For these alloys the silicon phase is segregated at the grain boundaries during solidification. From the figure, it is evident that 356CM-T61 and 356PM-T61 have similar microstructure which is due to the similarity of the fabrication and heat treatment processes. The 356DC-NT (Fig. 5c) has finer grain size which is due to the higher cooling rate during fabrication. In the non-treated 356CM-NT, the silicon phase is less dispersed and the silicon particles have irregular shape. Round silicon particles are characteristic for the heat treated alloys.

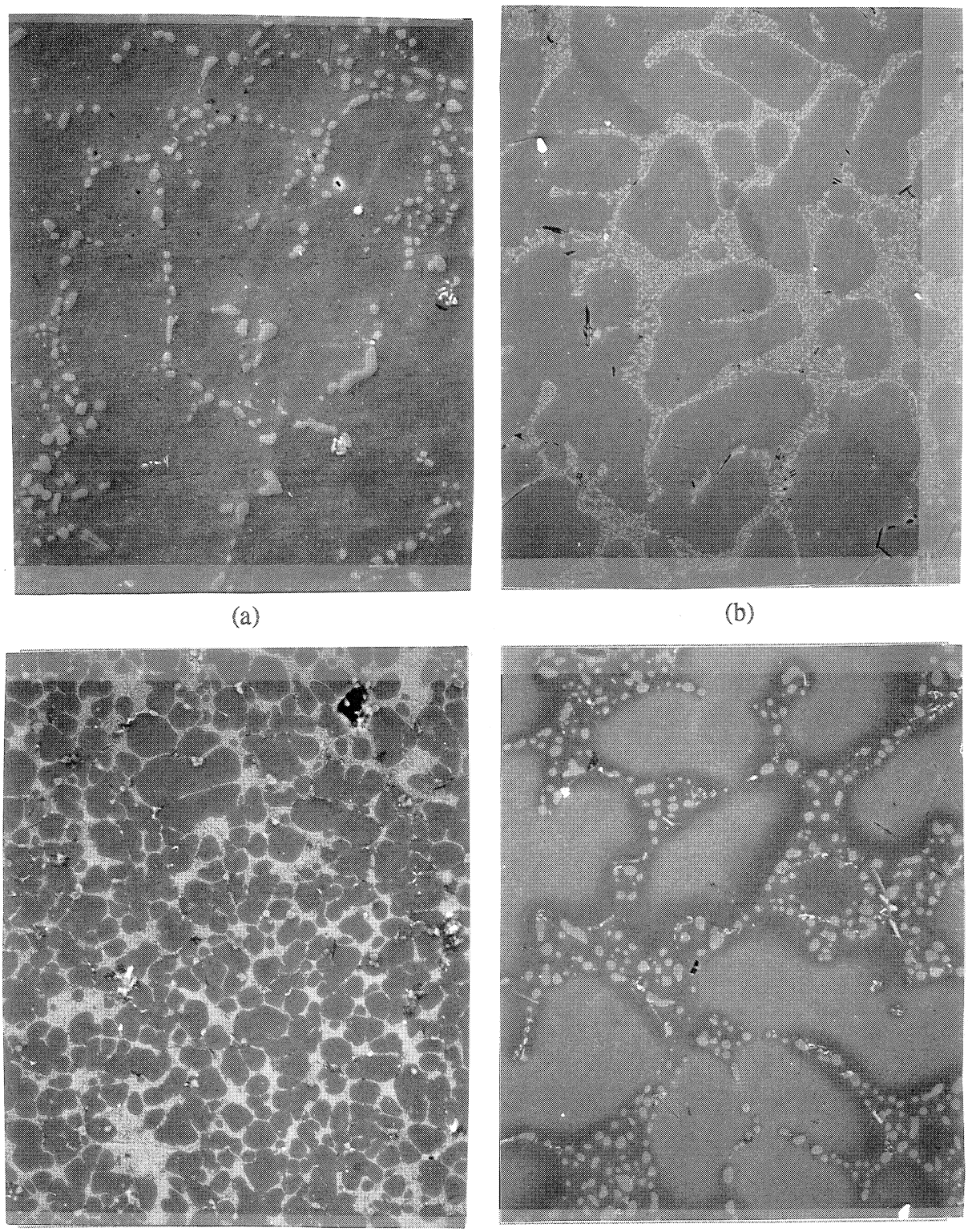

Fig. 5 - SEM Pictures of Microstructure of 356 alloys. Magnification 400x.
(a) 356CM-T61, (b) 356CM-NT, (c) 356DC-NT, (d) 356PM-T61

3.4 Test Conditions and Lubricants

Various test conditions and lubricant/refrigerant mixtures were used in this experimental program. Most of the tests were conducted at an environmental temperature of 38°C (100°F) and an environmental pressure of 0.86 MPa (125 psig). Some of the tests was conducted at an environmental temperature of 121°C (250°F) and an environmental pressure of 0.17 MPa (25 psig). The 38°C (100°F) temperature combined with the 0.86 MPa (125 psig) pressure is the high refrigerant content condition, while the 121°C (250°F) temperature and 0.17 MPa (25 psig) pressure is the low refrigerant content condition. With the exception of the hard anodized 356CM alloys (Hardcoat® and Nituff® in Table 1) and a SiC particle reinforced composite, a contact load of 111 N (25 lbf) was used. In order to get a measurable wear, a much higher load of 667 N (150 lbf) was used for the hard anodized alloys and the SiC composite. The sliding velocity of 0.209 m/s (41.3 fpm) was used for all tests conducted. Again, this sliding speed was chosen to get a measurable wear for the limited time of test duration. The designation of the test conditions and their description are given in Table 3.

Two esters which have similar viscosity were used with R134a, R407 or R410 refrigerants. Two PAGs which also have similar viscosity were used in R134a environment. A mineral oil and alkylbenzene were used with R22, R407 or R410 refrigerants. Data for the lubricants used are given in Table 4. The viscosity of various L/R mixtures used for given test conditions is measured using an in-line viscometer. The viscosity changes of various L/R mixtures with time are plotted in Fig. 6.

Table 3 - Test Conditions

Condition	Environment	Lubricant	L/R Viscosity cS	Env. Pressure MPa (psig)	Env. Temp. °C (°F)	Contact Load N (lbf)	Cont. Pressure MPa (ksi)
A	R134a	Ester 1	4.83	0.86 (125)	38 (100)	111 (25)	322 (46.7)
B	R134a	Ester 2	2.40	0.86 (125)	38 (100)	111 (25)	322 (46.7)
C	R134a	PAG 1	8.04	0.86 (125)	38 (100)	111 (25)	322 (46.7)
D	R134a	PAG 2	7.03	0.86 (125)	38 (100)	111 (25)	322 (46.7)
E	R22	Alkylbenzene	4.98	0.86 (125)	38 (100)	111 (25)	322 (46.7)
F	R22	Mineral Oil	4.98	0.86 (125)	38 (100)	111 (25)	322 (46.7)
G	R407C	Ester 1	10.67	0.86 (125)	38 (100)	111 (25)	322 (46.7)
H	R410A	Ester 1	13.35	0.86 (125)	38 (100)	111 (25)	322 (46.7)
I	R134a	Ester 1	3.32	0.17 (25)	121 (250)	111 (25)	322 (46.7)
J	R134a	PAG 1	6.62	0.17 (25)	121 (250)	111 (25)	322 (46.7)
K	R134a	Ester 1	5.73	0.86 (125)	38 (100)	667 (150)	1929 (280)
L	R407C	Ester 1	11.40	0.86 (125)	38 (100)	667 (150)	1929 (280)
M	R410A	Ester 1	16.10	0.86 (125)	38 (100)	667 (150)	1929 (280)
N	R407C	Alkylbenzene	14.05	0.86 (125)	38 (100)	111 (25)	322 (46.7)
O	R407C	Mineral Oil	7.97	0.86 (125)	38 (100)	111 (25)	322 (46.7)
P	R410A	Alkylbenzene	15.3	0.86 (125)	38 (100)	111 (25)	322 (46.7)
Q	R410A	Mineral Oil	9.36	0.86 (125)	38 (100)	111 (25)	322 (46.7)
R	Air	Ester 1	23.15	0.0 (0.0)	38 (100)	111 (25)	322 (46.7)

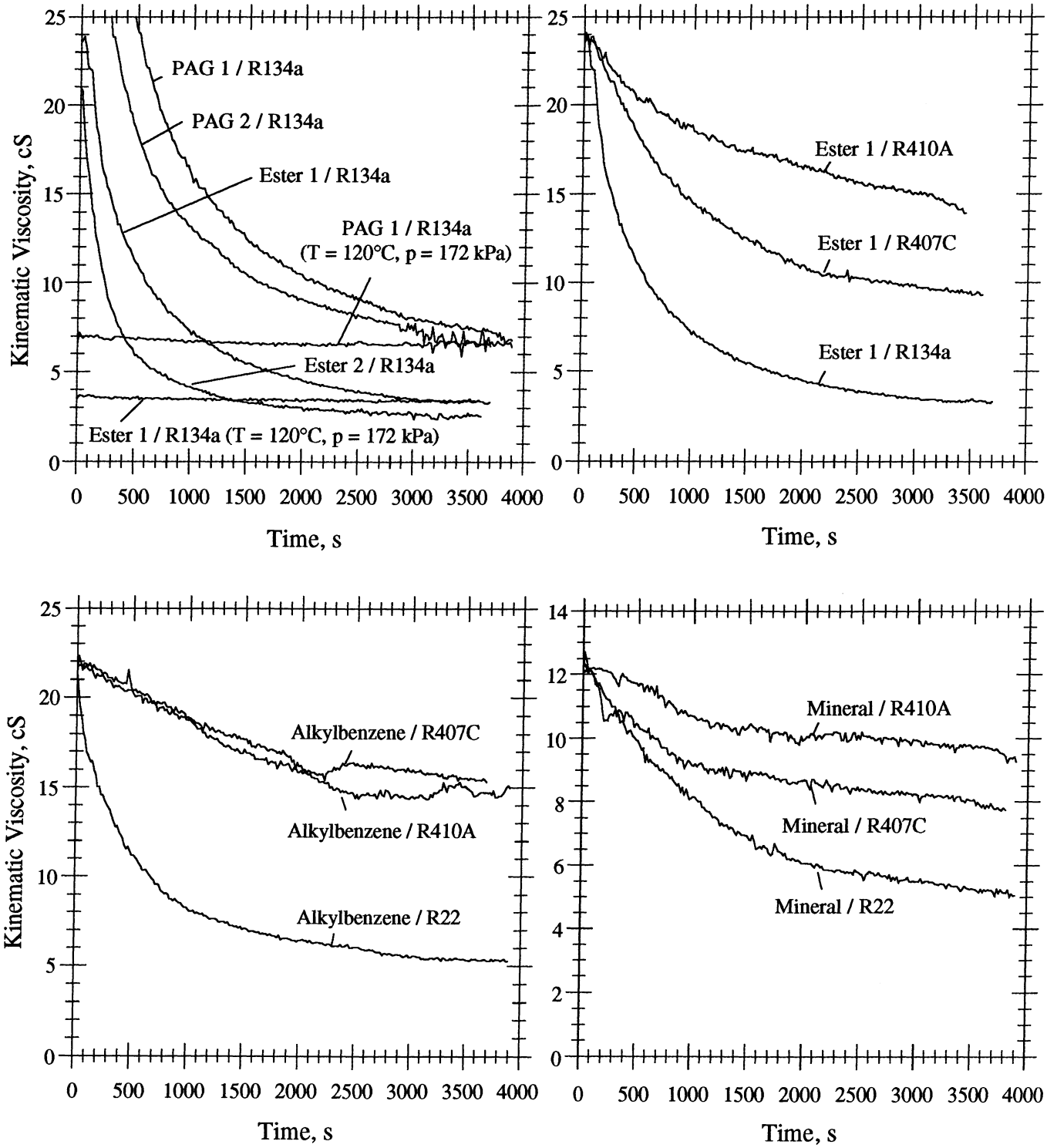

Fig. 6 - Viscosity of Various Lubricant/Refrigerant Mixtures vs. Time
T = 38°C, p = 860 kPa Unless Otherwise Noted.

Table 4 - Data for the Lubricants Tested

Designation	Lubricant Type	Family	Additives	Density g/ml	Viscosity, cS	
					at 40 °C	at 100 °C
Ester 1	Polyolester	Pentaerythritol	No	0.990	23.9	4.9
Ester 2	Polyolester	Pentaerythritol	Antioxidant	0.998	18.9	4.2
PAG 1	Polyalkylene glycol	Uncapped	No	0.990	49.5	9.8
PAG 2	Polyalkylene glycol	Capped	No	0.990	51.0	9.8
Alkylbenzene	Alkylbenzene		No	0.825	20.4	3.5
Mineral	Mineral oil		No	0.894	12.0	2.6

3.5 Test Procedure and Data Obtained

All tests were conducted in the pressure chamber of the HPT under copious lubrication condition (the contact pair was completely submerged in the L/R mixture) for the test duration of one hour. Whenever a test was conducted under a refrigerant environment, the refrigerant was charged into the pressure chamber and allowed to dissolve in the lubricant for one hour prior to initiating the test.

In order to examine the worn surfaces of the aluminum alloys, some specimens were sectioned and then examined with a scanning electron microscope (SEM). The surface of the test specimens was also examined with an X-ray photoelectron spectroscopy (XPS) to study and try to identify the chemical compounds formed on the surface. Metalographic samples of test specimens were also prepared to study the effect of heat treatments and the method of fabrication.

The coefficient of friction was monitored and recorded continuously throughout the test by a computer-based data acquisition system. The friction data shown in the results are average values. The wear on the aluminum specimens (discs) was obtained via a stylus surface profilometer by taking surface profiles and measuring the average wear scar depth. The wear on the steel pins was obtained by measuring the wear scar with an optical microscope. The wear scars on the pins were also examined with an optical microscope for material transfer from the aluminum counterface.

4. RESULTS

4.1 Materials Screening Tests

Various types of aluminum alloys were tested under lubricated sliding conditions. The friction and wear characteristics of these alloys were evaluated in a refrigerant environment. The friction and wear results obtained from the materials screening tests are given in Tables 5 and 6. Information about the average friction coefficient, the depth of the wear scar on the discs, the width of the wear scar on the pins, the average contact resistance, the roughness of the disc surface before and after the test, and a qualitative estimate (Fig. 8) of the amount of material transfer are also included in these tables.

Table 5 - Materials Screening at Condition A (Table 3)

R134a @ 0.86 MPa, T = 38°C, Ester 1 Lubricant, Viscosity of the L/R Mixture = 4.83 cS, Contact Load = 111N

Material Designation	Average Friction	Disc Wear Depth μm	Pin Wear Scar mm	Contact Resistance Ω	Wear Scar Roughness μm Ra	Roughness Before Test μm Ra	Amount of Material Transfer†
HV3-T6	0.123	1.11	0.23	~1-10	0.146	0.201	Medium
HV3-T4	0.150	1.10	0.27	~1-10	0.253	0.238	None
HV4-T61	0.129	1.02	0.23	0.95	0.164	0.162	None
C278-T4	0.203	1.32	0.26	~1-10	0.269	0.206	None
6061-T61	0.249	270	0.29	5.5×10^{-3}	0.492	0.485	Large
2024-T351	0.282	153	0.28	3.8×10^{-4}	0.429	0.490	Medium
390DC-T6	0.130	0.681	0.25	11.7	0.128	0.258	None
390PM-T61	0.122	0.936	0.22	3.39	0.135	0.275	None
356DC-NT	0.119	3.79	0.22	8.71	0.466	0.808	None
356PM-T61	0.116	1.98	0.23	0.38	0.695	0.0946	Medium
356CM-T61	0.126	1.95	0.22	4.24	0.538	0.159	Medium
356CM-NT	0.132	1.84	0.27	4.3×10^{-3}	0.207	0.181	Small
356CM-AN	0.164	7.89	0.20	6.5×10^{-3}	1.381	0.199	Medium

† See Fig. 8

Table 6 - Materials Screening at Condition C (Table 3)

R134a @ 0.86 MPa, T = 38°C, PAG 1 Lubricant, Viscosity of the L/R mixture = 8.04 cS, Contact Load = 111 N

Material Designation	Average Friction	Disc Wear Depth μm	Pin Wear Scar mm	Contact Resistance Ω	Wear Scar Roughness μm Ra	Roughness Before Test μm Ra	Amount of Material Transfer †
HV3-T6	0.111	3.40	0.21	1.1	0.339	0.212	Medium
HV3-T4	0.118	3.39	0.21	~0.1-1.0	0.430	0.206	Medium
HV4-T61	0.085	2.37	0.18	0.21	0.172	0.147	None
C278-T4	0.129	2.27	0.18	14.8	0.242	0.215	Medium
6061-T61	0.205	87.6	0.19	3.0×10^{-2}	0.492	0.485	Large
2024-T351	0.269	221	0.36	9.3×10^{-4}	0.567	0.495	None
390DC-T6	0.132	1.11	0.16	3.2	0.100	0.238	None
390PM-T61	0.140	1.82	0.18	2.0	0.160	0.170	None
356DC-NT	0.155	46.7	0.30	3.3×10^{-2}	1.23	0.665	Large
356PM-T61	0.116	5.47	0.22	0.25	0.472	0.125	Large
356CM-T61	0.117	7.37	0.25	4.48	0.394	0.170	Large
356CM-NT	0.108	6.76	0.21	3.31	0.320	0.217	Large
356CM-AN	0.167	11.4	0.19	1.5×10^{-3}	0.983	0.222	None

† See Fig. 8

With the exception of the 6061-T61 and 2024-T351 alloys, the wear depth on the aluminum discs is also given in Fig. 7 for conditions A and C. Since the wear obtained with the 6061-T61 and 2024-T351 alloys was much higher than that of other alloys, the wear results of these alloys are not plotted in this figure. This figure also shows the scatter of the test data. It should be noted that there is more scatter with 356 alloys. This is mainly due to the relatively severe surface fatigue (or delamination) of these alloys which could not be controlled from test to test. In general, there is more scatter when more surface fatigue occurred on the surfaces. The surface fatigue phenomenon will be discussed in more detail in section 4.4. Examples of various amounts of material transfer are provided in Fig. 8.

The load under conditions A and C was insufficient to cause measurable wear on the SiC-Al composite and on the specimens with hard anodized coating. Therefore, these materials were tested at six times higher load (condition K in Table 3). The substrate material for the hard anodizing coatings (356CM-T61) was also tested at higher load for comparison purpose. The friction and wear results from these higher load tests are given in Table 7. These results are also plotted in Fig. 9.

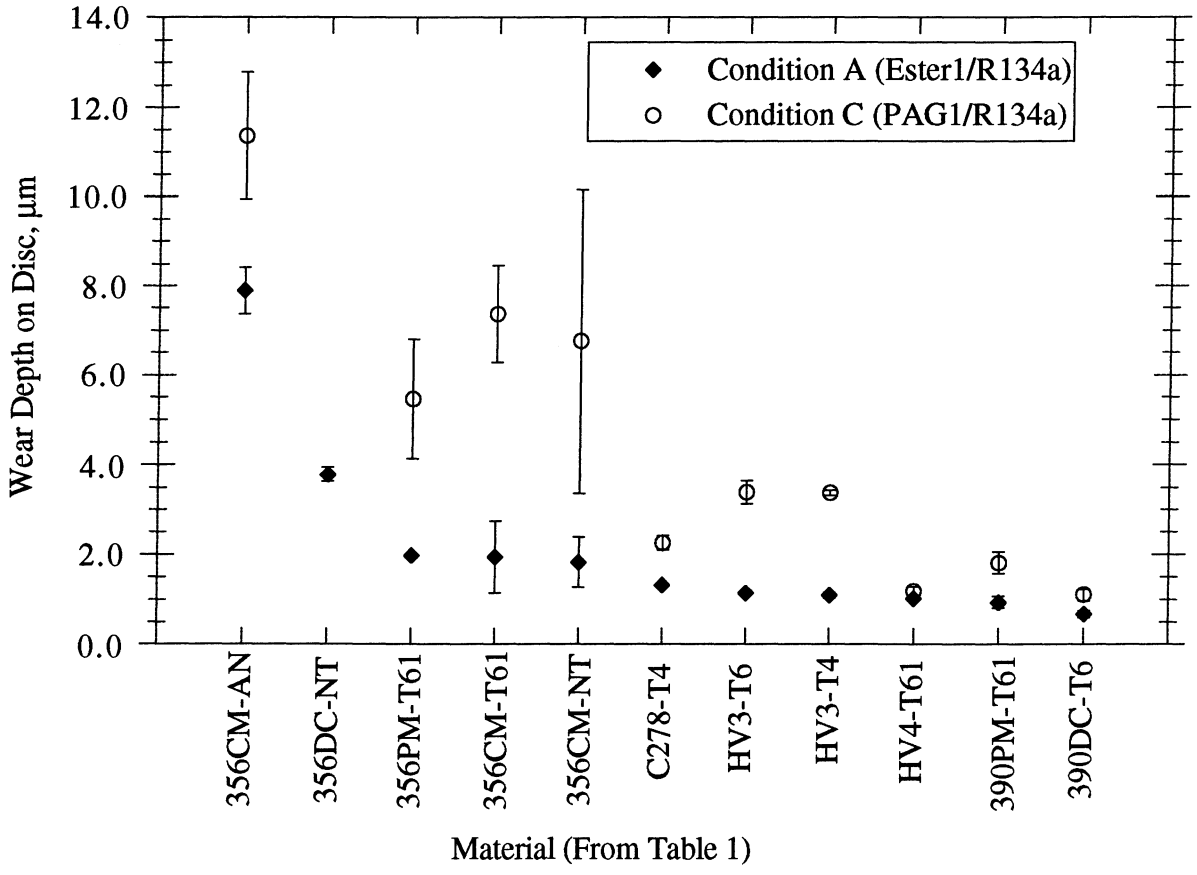

Fig. 7 - Wear Results for Various Aluminum Alloys under Conditions A and C

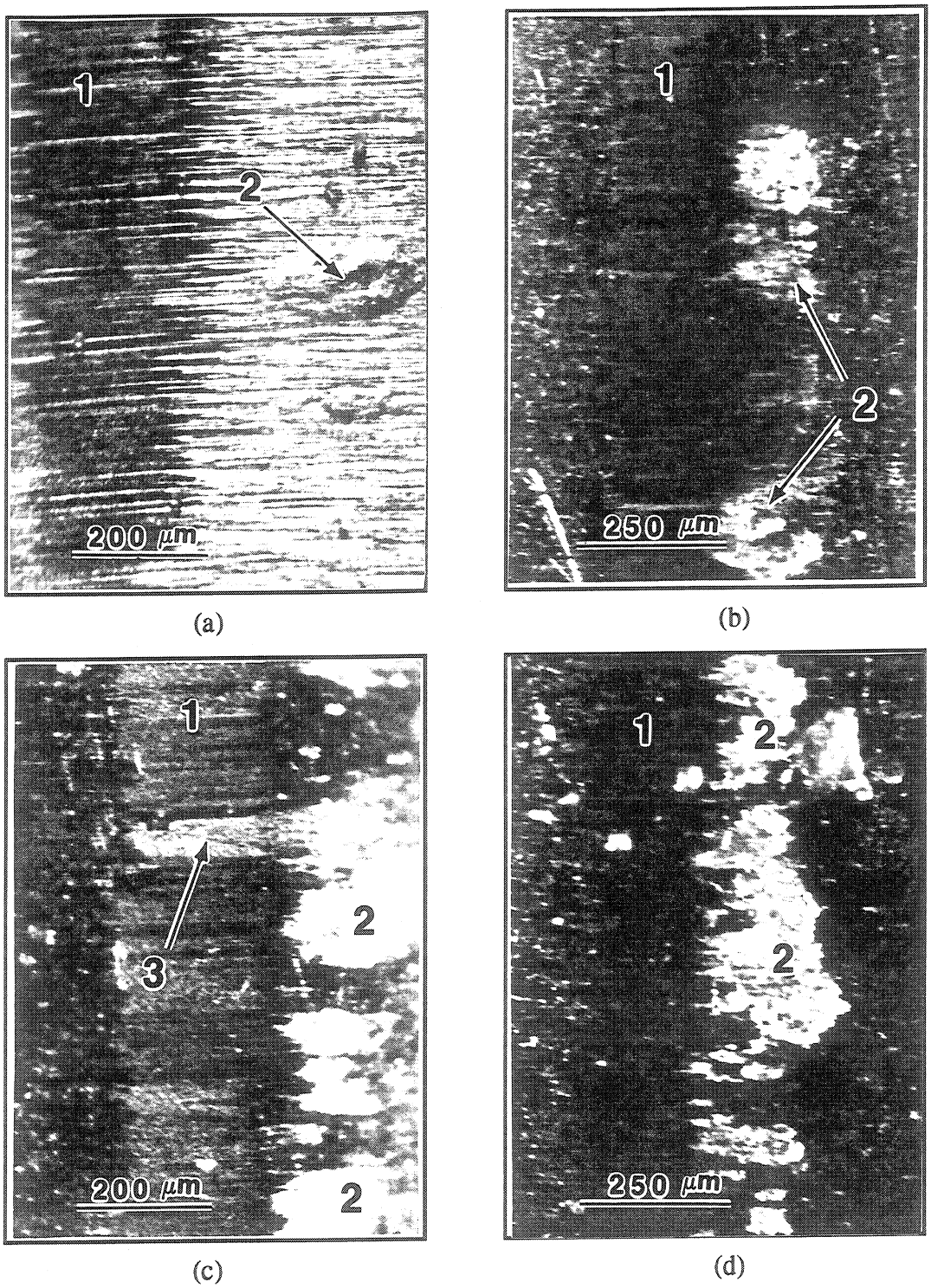

Fig. 8 - Examples of Aluminum Transfer to the 1018 Steel Pins
The Direction of Sliding is from Right to Left
1 - Wear Scar, 2 - Transfer Agglomeration, 3 - Material Smeared on the Wear Scar
(a) Small Transfer - Single Spot, (b) Medium Transfer - Several Spots, (c) Large Transfer - Continuous Band and a Smeared Particle, (d) Large Transfer - Continuous Band

Table 7 - Materials Screening at Condition K

(R134a @ 0.86 MPa, Ester 1 Lubricant, T = 38°C, Viscosity of the L/R mixture = 4.83 cS, Contact Load = 667N)

Material	Treatment	Average Friction	Disc Wear Depth µm	Pin Wear Scar mm	Contact Resistance Ω	Wear Scar Roughness µm Ra	Roughness Before Test µm Ra	Amount of Material Transfer †
356CM-T61	T61	0.099	9.78	0.36	3.85	0.47	0.15	Large
356CM-HC	Hardcoat®	0.122	1.59	0.75	~10^{+4}	2.01	2.72	None
356CM-NF	Nituff®	0.124	1.93	0.75	~10^{+4}	1.98	2.71	None
SiC-Al		0.121	2.15	1.10	2.57×10^{-5}	0.39	0.42	None

† See Fig. 8

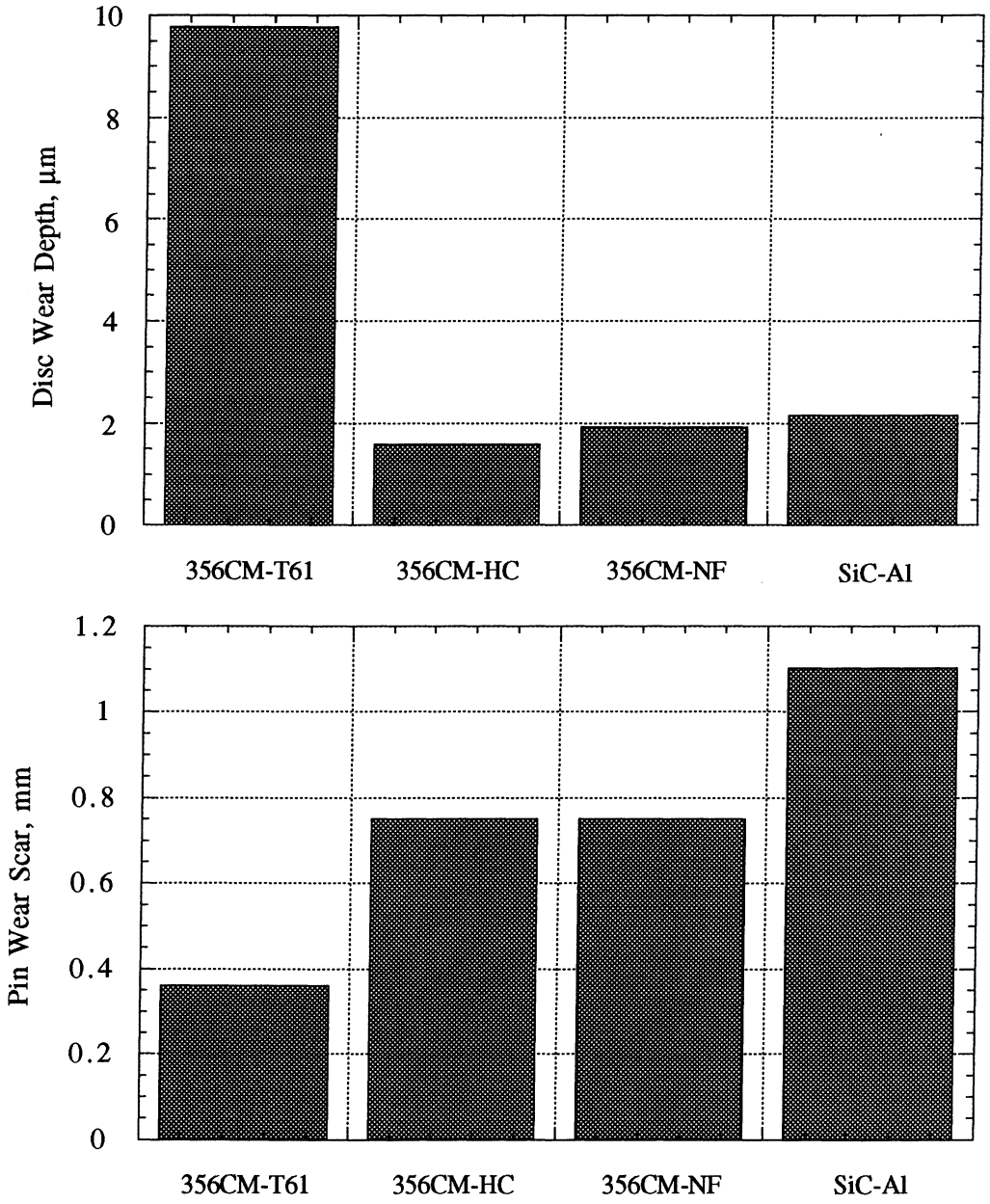

Fig. 9 - Wear Results at Condition K

From the wear results given in Fig. 7, it is seen that the Ester/R134a mixtures consistently provided better protection of the aluminum disc specimens compared to the PAG/R134a mixtures, even though the viscosity of the Ester/R134a mixture is lower than that of the PAG/R134a mixture. This effect is probably due to the ability of the esters to form bidentate bonds with aluminum [35, 36]. Note that the wear result of 356DC-NT at condition C is not given in Fig. 7. Excluding the 6061-T61 and 2024-T351 alloys, the 356DC-NT has approximately one order of magnitude higher wear than the other materials tested. A relatively large material transfer is observed for this alloy tested at condition C. Conventional anodizing (356CM-AN) does not improve the wear resistance of the 356 aluminum alloy under concentrated contacts. The hard layer cracks under the high contact stress causing an increase in wear. The lowest wear is obtained with the 390DC-T6 alloy which also has the highest hardness. In general, the amount of wear decreases as the amount of silicon content increases. This trend, however, is complicated by the presence of other alloying elements and the different treatment processes. A comparison between the HV3 and 356, which have similar Si contents, indicates that the HV3 consistently provided better wear resistance. The reason for the improved performance of HV3 is either the higher Cu content, or the presence of Bi. Similar conclusions can be drawn when comparing the results for C278-T4 and HV4-T61. Even though the C278-T4 and HV4-T61 have the same amount of Si, HV4-T61 is more wear resistant due to the higher Cu and Bi contents. While copper is known to provide better wear resistance, it is still not clear what is the effect of bismuth due to other alloying elements. From the wear results given in Fig. 9, it can be seen that hard anodizing and SiC particle reinforcement provide very good wear resistance. However, they cause increased wear on the counterface due to the rough hard surfaces generated by hard anodizing processes and the hard SiC particles on the surface of a SiC-Al composite.

Aluminum alloys are notorious for their material transfer to the counterface. Under the conditions of this study, the material transfer to the steel pins took the form of particle agglomeration at the inlet of the sliding contact (Fig. 8). In most cases, however, the contact surface of the steel pin was free from transferred material, and only occasionally a particle was smeared on the wear scar (Fig. 8c). The agglomeration of transferred material at the inlet of the contact suggests that the geometry of the contact has a significant effect on this process. It seems that contacts with converging wedge geometries are more prone to material transfer. When wear increases, material transfer also tends to increase, although the relationship is probably quite complex. In the cases when large wear particles were generated (for example when the 356 alloy suffered surface fatigue), the transfer was also large.

The roughness of the wear scar is an indicator of the severity of the wear damage as well as the wear mechanism. The roughness of the 390 alloys, for example, decreased during the test. These were also the alloys with the least wear. The value of the roughness in this case suggests that the materials operated in the mild wear regime. The roughness of the 356 discs (with the exception of 356CM-NT) increased significantly due to the delamination wear mechanism. The wear scar was generally smoother

under condition A (Ester 1/R134a) compared to condition C (PAG 1/R134a) which correlates well with the corresponding wear.

As mentioned earlier, the electrical contact resistance can also be an indicatior of the condition at the contact. The contact resistance (R) of a single junction is given in [42] as:

$R = R_1 + R_2 + R_f$, where $R_1 = \frac{\rho_1}{4a}$, $R_2 = \frac{\rho_2}{4a}$, R_f is the resistance of surface films, ρ_i are the resistivities of the materials, and a is the diameter of the junction. If it is assumed that $R_f = 0$ (adhesion of clean metals), the diameter of a junction can be estimated, if R is known. Real surfaces make contact at numerous spots with non circular shape, vastly complicating the problem. In addition, certain conductance through the boundary films also occurs. However, an upper bound for the clean metal contact area can be obtained if it is assumed that the conductance is due to a single contact spot and the effect of the boundary films is neglected. In this case, the area over which metal contact occurs is given by:

$$A_a = \frac{\pi a^2}{4}$$

The resistivities of aluminum and steel are 2.8×10^{-8} Ωm and 15.8×10^{-8} Ωm, respectively. The apparent contact area (A) for most cases in this study was approximately 1.5 mm^2. Making use of the above assumptions, the values of A_a/A are given in Table 8. This approach can only be applied to cases where A_a/A is small and it fails at $R \leq 10^{-5}$ Ω.

Table 8 - Estimates of the Area Over Which Metal Contact Occurred

Measured Resistance Ω	Diameter of the Contact mm	Area of the Contact Spot mm^2	A_a/A %
1	4.7×10^{-5}	1.7×10^{-9}	1.13×10^{-7}
10^{-1}	4.7×10^{-4}	1.7×10^{-7}	1.13×10^{-5}
10^{-2}	4.7×10^{-3}	1.7×10^{-5}	0.00113
10^{-3}	4.7×10^{-2}	1.7×10^{-3}	0.113
10^{-4}	0.47	0.17	11.3

Under the conditions of this study, the static contact of steel against aluminum had a contact resistance of the order of 10^{-3} Ω, which, as seen from Table 8, roughly corresponds to only 0.11% metal contact. An average contact resistance higher than this value indicates the formation of boundary films during sliding. A resistance of the order of 1Ω, which is typical for most of the tests, indicates that the metal contact in these cases was negligible. On the other hand, a resistance in the range 10^{-5}-10^{-4}Ω, indicates that metal contact occurs on a significant portion of the contact area. Occasional downward spikes in the contact resistance (Fig. 4) were characteristic for the cases when large material transfer occurred and are probably due to debris transfer agglomerations passing through the contact (Fig. 8c).

4.2 Friction and Wear of 356CM-T61 and 390PM-T61 under Various Conditions

These two Al-Si alloys, which are widely used in critical components of refrigerant compressors, were examined for their friction and wear behavior in different L/R mixtures and at various operating and environmental conditions. Table 9 and 10 show results obtained under various L/R combinations and test conditions. Note that tests at conditions K, L and M were not conducted with 390PM-T61 alloy. Results for the wear depth on the aluminum discs under selected conditions are also plotted in Fig. 10.

Table 9 - Results for 356-T61 Coupon Mold Aluminum Alloy Tested under Various Conditions

Condition (Table 3)	Average Friction	Disc Wear Depth μm	Pin Wear Scar mm	Contact Resistance Ω	Wear Scar Roughness μm Ra	Roughness Before Test μm Ra	L/R Viscosity cS	Amount of Material Transfer †
A	0.121	1.71	0.22	4.24	0.498	0.179	4.83	Medium
B	0.123	3.14	0.24	9.17	1.260	0.136	2.40	Medium
C	0.117	7.37	0.28	N.A.	0.394	0.143	8.04	Large
D	0.119	3.54	0.21	9.3	0.310	0.127	7.03	Small
E	0.103	1.57	0.26	6.26	0.184	0.170	4.98	None
F	0.106	0.85	0.28	2.05	0.181	0.155	4.98	None
G	0.114	1.83	0.17	0.90	0.194	0.105	10.67	Small
H	0.127	1.86	0.16	1.69	0.229	0.130	13.35	None
I	0.118	2.15	0.22	4.69	0.162	0.092	3.32	Small
J	0.075	4.22	0.26	4.48	0.442	0.201	6.62	Medium
K	0.099	9.78	0.35	0.51	0.472	0.107	5.73	Medium
L	0.098	5.71	0.31	2.36×10^{-2}	0.356	0.098	11.40	None
M	0.088	5.27	0.30	2.74×10^{-3}	0.435	0.089	16.10	None
N	0.114	1.13	0.27	1.77	0.226	0.139	14.05	None
O	0.132	1.07	0.18	3.57	0.152	0.128	7.97	None
P	0.108	1.26	0.25	3.43	0.373	0.164	15.3	None
Q	0.117	1.37	0.21	3.3×10^{-2}	0.287	0.182	9.36	None
R	0.112	2.05	0.13	9.75	0.136	0.132	23.15	None

† See Fig. 8

Table 10 - Results for 390-T61 Permanent Mold Aluminum Alloy Tested under Various Conditions

Condition (Table 3)	Average Friction	Disc Wear Depth μm	Pin Wear Scar mm	Contact Resistance Ω	Wear Scar Roughness μm Ra	Roughness Before Test μm Ra	L/R Viscosity cS	Amount of Material Transfer †
A	0.128	0.86	0.23	0.37	0.225	0.160	4.83	None
B	0.139	1.58	0.26	8.70	0.262	0.165	2.40	None
C	0.140	1.82	0.18	2.00	0.160	0.170	8.04	None
D	0.166	1.80	0.19	11.3	0.141	0.165	7.03	None
E	0.116	0.97	0.20	8.94	0.117	0.113	4.98	None
F	0.136	1.03	0.23	8.96	0.136	0.200	4.98	None
G	0.116	0.88	0.20	0.16	0.165	0.116	10.67	None
H	0.120	0.74	0.21	3.9×10^{-3}	0.159	0.178	13.35	None
I	0.096	1.25	0.34	5.00	0.180	0.146	3.32	None
J	0.134	1.42	0.36	6.22	0.213	0.190	6.62	None
N	0.122	1.09	0.20	7.20	0.089	0.191	14.05	None
O	0.147	0.78	0.22	2.96	0.092	0.215	7.97	None
P	0.102	0.96	0.21	4.94	0.124	0.127	15.3	None
Q	0.100	1.25	0.20	3.41	0.118	0.199	9.36	None
R	0.092	1.20	0.28	10.7	0.165	0.216	23.15	None

† See Fig. 8

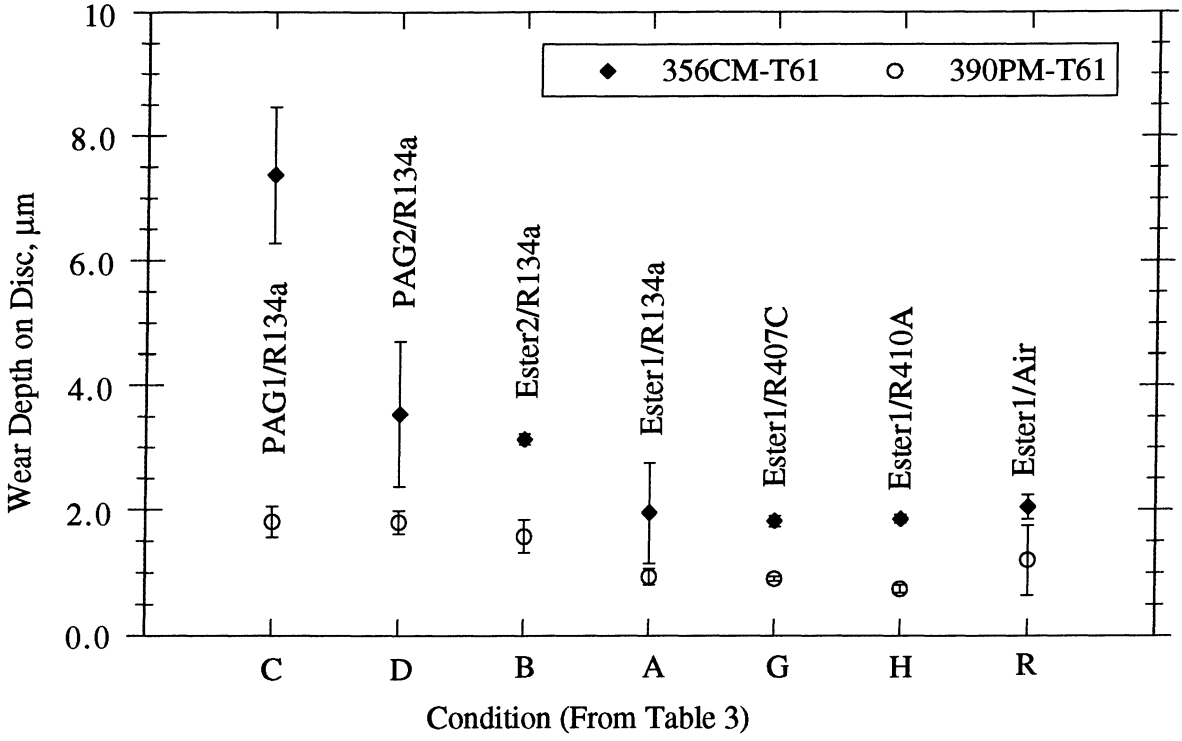

Fig. 10 (a) - Wear Results for Ester and PAG Lubricants in Various Environments

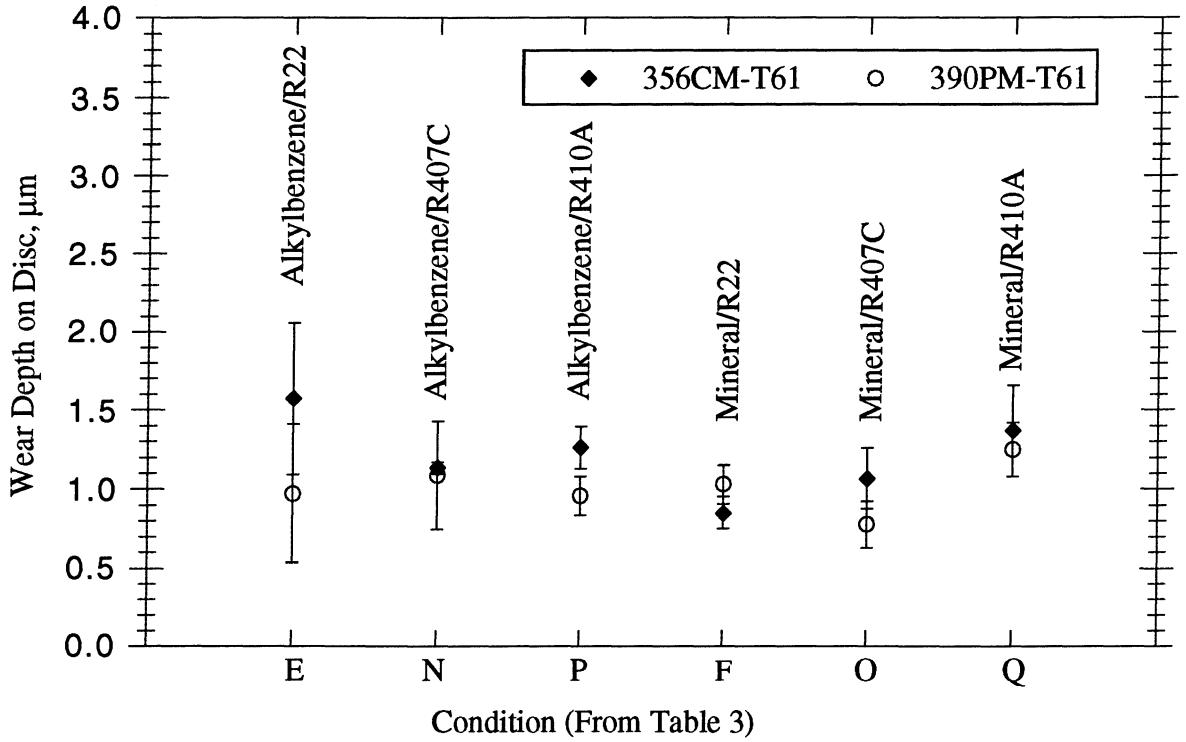

Fig. 10 (b) - Wear Results for Alkylbenzene and Mineral Oil in R22, R407C and R410A

From the wear results shown in Fig. 10, it is seen that, with the exception of condition F, the wear depths on 390PM-T61 alloy were consistently smaller than those on 356CM-T61 alloy. The capped PAG (PAG 2) provides better lubricity for 356CM-T61 alloy than the uncapped lubricant (PAG 1). However, for the 390PM-T61 alloy, the lubricity of the PAG's is about the same. When Ester 1 lubricant is used, the wear on the discs for both alloys is about the same in R134a, R407C, R410A and air environments. The R407C and R410A used with alkylbenzene lubricant provide similar (with 390PM-T61) or slightly better (with 356CM-T61) wear resistance when compared to R22. The lower wear obtained with the 356CM-T61 alloy is probably due to the higher viscosity of alkylbenzene/R407C or R410A mixtures compared to the alkylbenzene/R22 mixture (Fig. 6). However, the relative wear differences between these mixtures are small, therefore, more tests need to be conducted to examine their lubricity difference, if any exists. The mineral/R22 mixture produces less wear (with 356CM-T61) than the other mixtures, even though the viscosity of the mineral/R22 mixture is smaller than that of the other mixtures (Fig. 6). However, with the 390PM-T61, it is the mineral/R407C mixture which provides slightly better wear resistance compared to the other mixtures. Again, the relative wear differences between these mixtures are not significant.

4.3 Effect of the Initial Surface Roughness on the Friction and Wear of 390 Aluminum

Both 390PM-T61 and 390DC-T6 discs were tested with different initial surface roughnesses. The results from these tests are given in Table 11. From the table, it is seen that, with 390DC-T6 under condition A, the surface with the lower roughness had also less wear. The surface roughness did not affect the results when the test was conducted under condition C. The material transferred from the smoother surface to the counterface under condition C was probably responsible for the slightly higher wear. Due to the scatter of the wear data obtained with 390PM-T61 under condition A, the surface roughness effect on this material is not obvious. More tests need to be conducted in order to get statistically significant result. The differences in the surface roughness of the wear scar are smaller than the differences in the initial (virgin) surface roughness. Under the conditions tests conducted, the results suggest that there is a trend towards an equilibrium condition of the surface, irrespective of its initial condition.

Table 11 - Effect of the Initial Disc Surface Roughness on 390 Alloy

Alloy	Condition	Initial Roughness μm Ra	Wear Scar Roughness μm Ra	Average Friction	Disc Wear Depth μm	Pin Wear Scar mm	Contact Resistance Ω	Amount of Material Transfer †
390DC-T6	A	0.258±0.009	0.129	0.130	0.681±0.074	0.25	11.7	None
390DC-T6	A	0.026±0.009	0.080	0.151	0.302±0.099	0.25	4.27	None
390DC-T6	C	0.259±0.015	0.010	0.132	1.11±0.12	0.16	3.17	None
390DC-T6	C	0.019±0.001	0.075	0.133	1.20±0.46	0.24	5.60	Medium
390PM-T61	A	0.191±0.028	0.225	0.128	0.859±0.017	0.23	0.37	None
390PM-T61	A	0.039±0.011	0.209	0.137	0.696±0.198	0.29	5.60	None
† See Fig. 8								

4.4 Surface Morphology and Wear Mechanisms

For the 356CM-T61 and 356PM-T61 alloys tested under a R134a refrigerant environment, extensive surface fatigue (delamination) was present, as shown in Fig. 11. Surface fatigue was not observed when the 356 alloys were tested in an air, R410A, or R407C environments. It was initially hypothesized that this behavior was due to lower viscosity L/R mixtures obtained with R134a which could cause hydrostatically accelerated cracking due to the deeper penetration of these mixtures in preexisting cracks and pores. However, this hypothesis fails to explain the fact that surface fatigue was not present when the viscosity of the L/R mixture was low due to higher temperature (conditions I and J from Table 3). Also, an examination of cross sections of worn and virgin surfaces (Fig. 12) with SEM did not reveal any preexisting cracks. For a contact load of 111 N, surface fatigue or cracks were observed only on the surfaces tested under R134a with high environmental pressure (0.86 MPa). The SEM examination did not reveal any plastically deformed or work-hardened layer, which is common for tests conducted under boundary lubricated conditions [9, 10]. Hence, excessive plastic deformation could not be the reason for surface cracking.

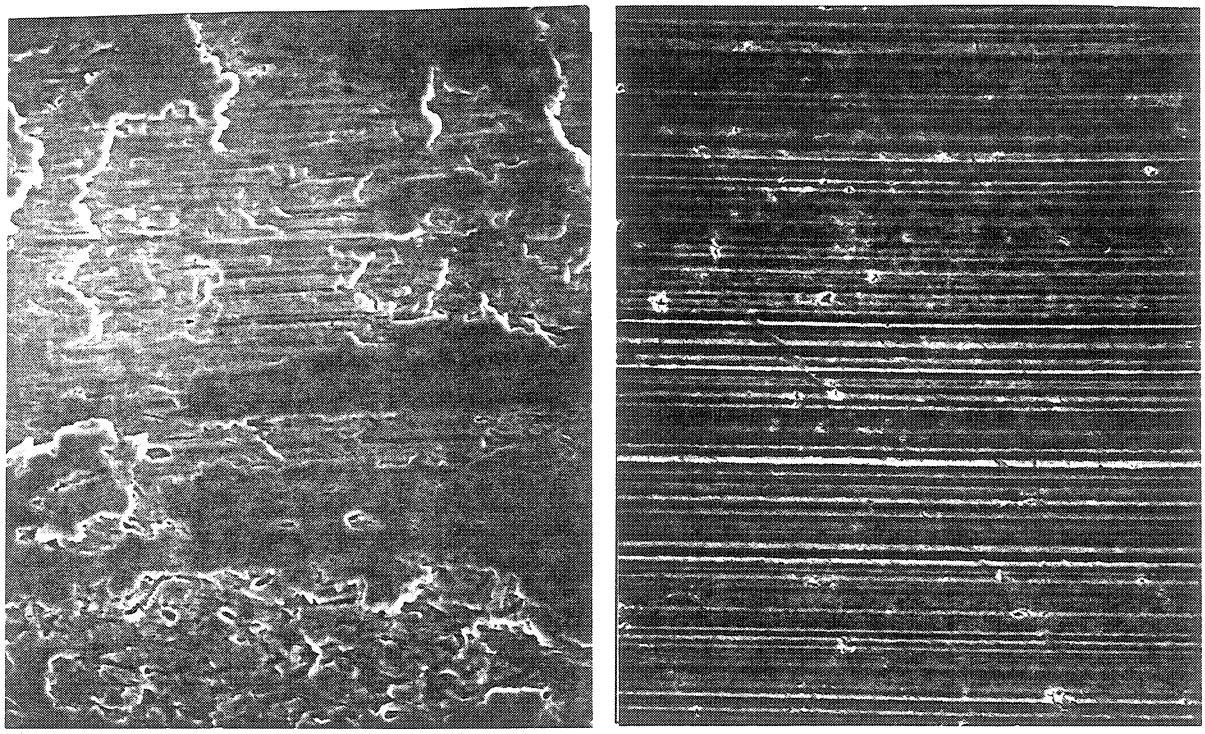

(a) (b)

Fig. 11 - SEM Micrographs of the Worn Surfaces of 356CM-T61 Alloy Tested Under (a) R134a and (b) Air Environments

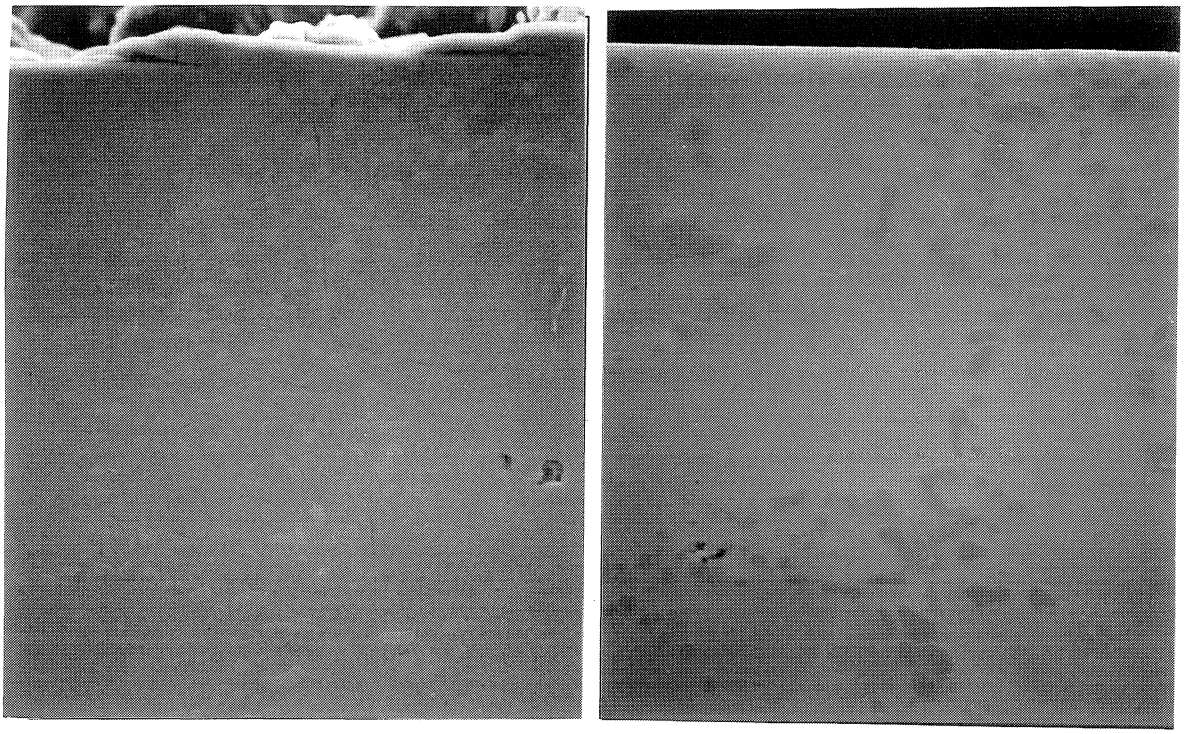

(a) (b)

Fig. 12 - SEM Micrographs of Cross Sections of 356 Alloy
(a) Worn Surface (b) Virgin Surface

Accelerated cracking due to the presence of the refrigerant may be a possible reason for the observed fatigue behavior. To explore this possibility, a set of tests at various environmental pressures was conducted with an Ester 1/R134a mixture. To exclude any effects due to the viscosity of the L/R mixture, the viscosity was kept approximately the same by changing the environmental temperature. The results from these tests are given in Table 12.

Table 12 - Effect of the Environmental Pressure of R134a on Surface Fatigue of 356-T61 Alloys

Environmental Pressure, MPa (psig)	0.17 (25)	0.52 (75)	0.69 (100)	0.86 (125)
Environmental Temperature, °C (°F)	121 (250)	100 (212)	80 (176)	38 (100)
Approx. Amount of R134a by Weight	3 %	8 %	13 %	50 %
Viscosity of the L/R Mixture, cS	3.33	4.24	4.69	4.85
Surface Fatigue	No	No	Small	Large

From the table, it is evident that at an environmental pressure of 0.69 MPa or higher, surface fatigue occurs. In addition to the above tests, a test in R407C (50% R134a, 25% R32, 25% R152a) at an environmental pressure and temperature of 0.86 MPa and 80°C, respectively was conducted. For this test, the L/R mixture had a viscosity of 5.14 cS. No surface fatigue was observed under these conditions. To completely exclude the effect of the lubricant, dry tests in R134a at environmental

pressure of 0.86 MPa and air at atmospheric pressure were also conducted. Due to the increased severity of the test conditions, the contact load was reduced to 44.4 N. The worn surfaces of the discs are shown in Fig. 13. From the figure, the surface tested in R134a seems to exhibit enhanced brittleness compared to the surface tested in air.

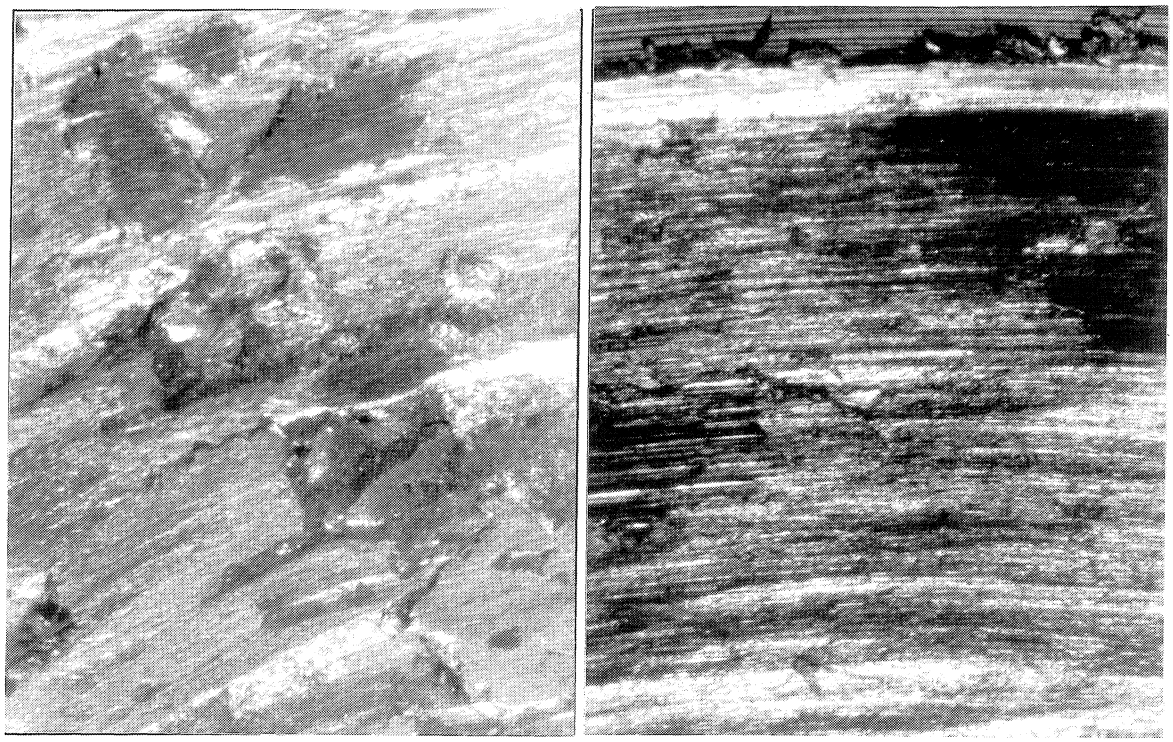

(a) (b)

Fig. 13 - Photographs of the Worn Surfaces of the 356CM-T61 Alloys
(a) Dry Test Under R134a Environment and (b) Dry Test Under Air Environment

Two distinct features were observed for the surface worn in an R134a environment (Fig. 14): (a) dark spots, which represented the load bearing area, and (b) metallic spots, which were formed by delamination of a wear particle. Both of these spots were examined with secondary ion mass spectroscopy (SIMS) in order to obtain the depth profiles for various chemical elements. For comparison purposes, a depth profile of the virgin surface was also made. The SIMS profiles are shown in Fig. 15. From the figure, it can be seen that both hydrogen and fluorine were present to a significant depth on the worn surface. The amount of these elements, at larger depths, is orders of magnitude higher than on the virgin surface. Additional study of the surface with X-ray photoelectron spectroscopy (XPS) revealed that the fluorine was in the form of AlF_3 (Fig. 16). It is hypothesized that the presence of hydrogen causes surface fatigue due to hydrogen embrittlement, while fluorine may cause corrosion cracking. No direct evidence for either of these possible mechanisms has been found so far. However,

based on the observation, an important conclusion that can be drawn from these studies is that R134a attacks the aluminum surface and enhances its brittleness.

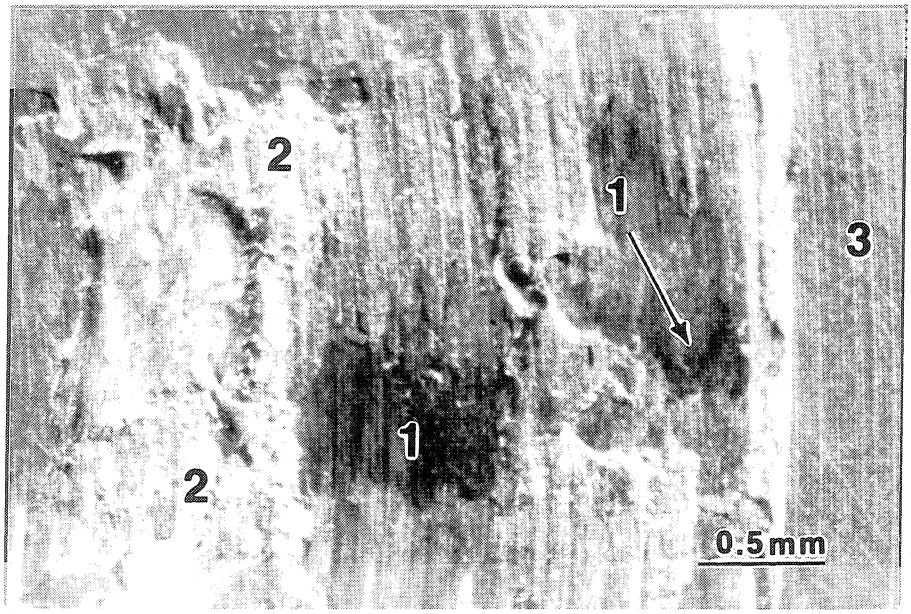

Fig. 14 - Photograph of the 356CM-T61 Alloy Tested Under Dry Conditions in R134a. Direction of Sliding: From Top to Bottom. 1 - Load Bearing Area, 2 - Bare Metal Generated by Delamination, 3 - Virgin Surface

Signs of surface fatigue, although much less severe, were also noted with some of the other alloys tested under condition C. Surface fatigue phenomena were also observed on 356CM-T61 tested under conditions L and M in Table 3 (higher contact load and different refrigerant). This suggests that the mechanism for this behavior is more general and not limited to the 356-T61 alloy. A XPS analysis of the worn disc surfaces tested under condition A showed that some decomposition of R134a had occurred, since AlF_3 was found on the surface. This indicates that the R134a refrigerant does not always behave as an inert compound, as previously thought [39-41]. As previously stated, a reaction between freshly exposed aluminum and R134a, leading to the formation of AlF_3, may be a possible reason for the enhanced brittleness. However, the actual causes and mechanisms for the surface fatigue on the 356 alloys are not clear at this time.

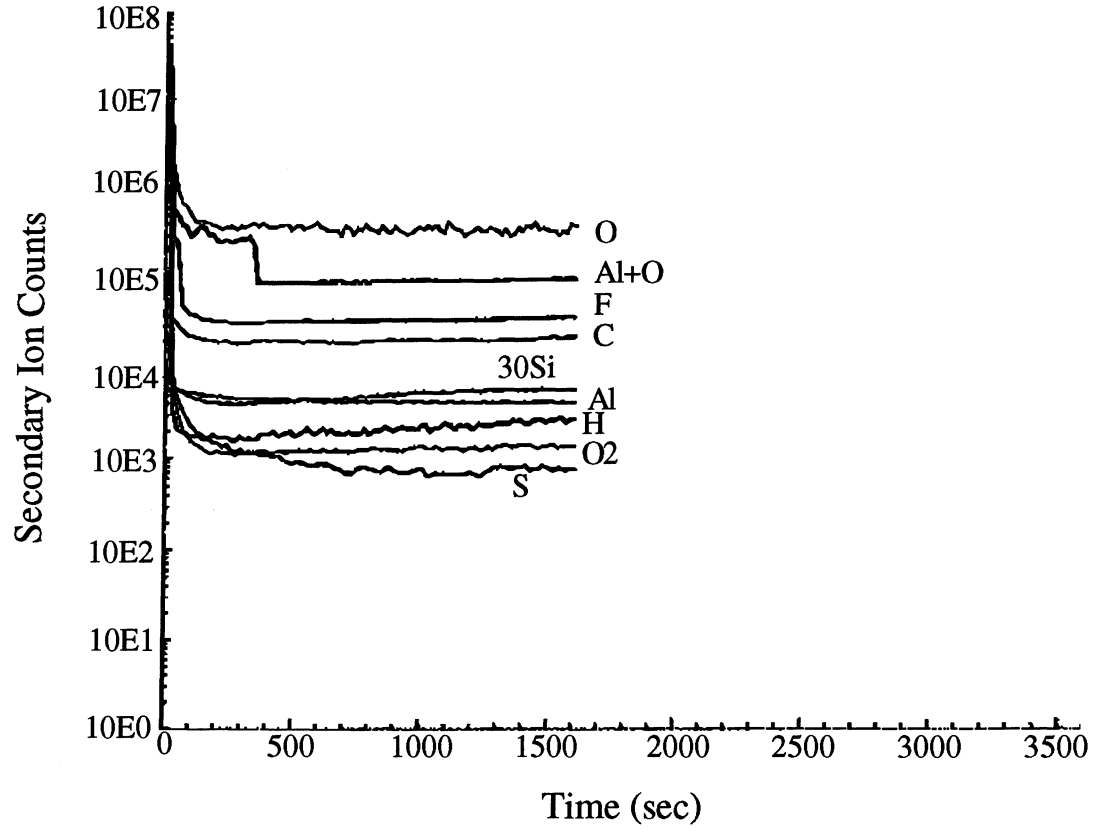
10E8
10E7
10E6
10E5
10E4
10E3
10E2
10E1
10E0
Secondary Ion Counts
O
Al+O
F
C
30Si
Al
H
O2
S
0
500
1000
1500
2000
2500
3000
3500
Time (sec)

(a)

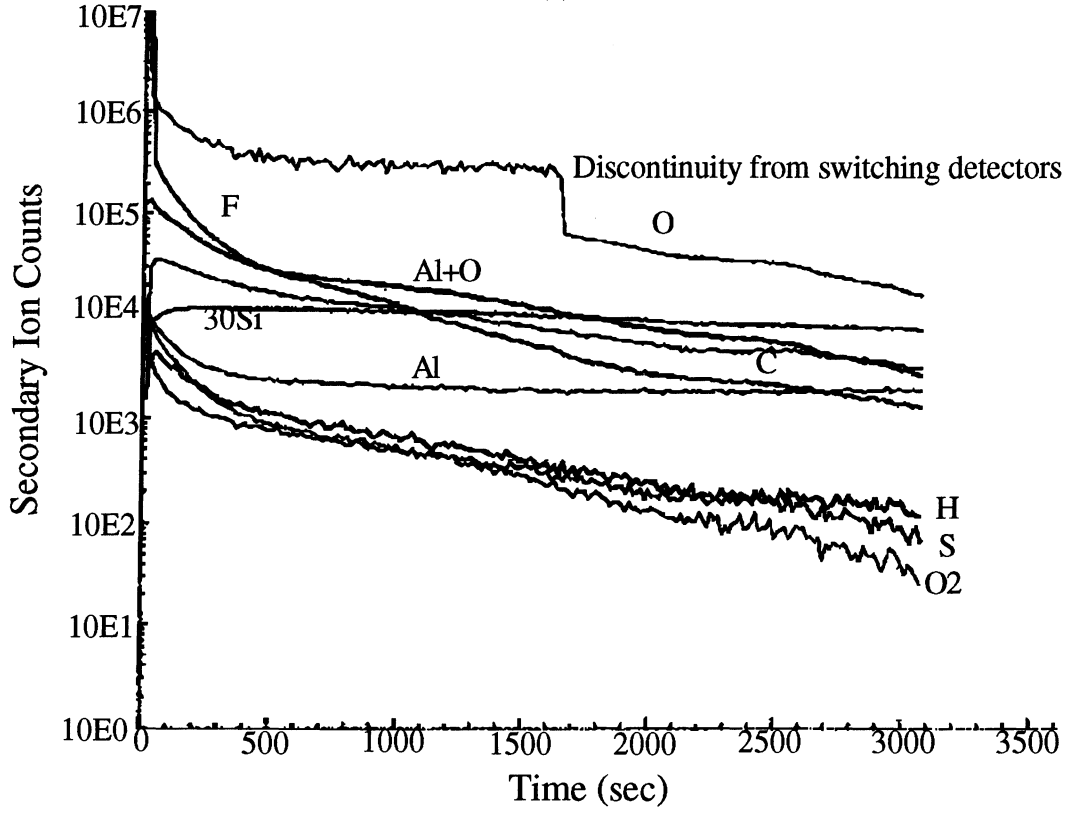
10E7
10E6
10E5
10E4
10E3
10E2
10E1
10E0
Secondary Ion Counts
Discontinuity from switching detectors
F
O
Al+O
30Si
Al
C
H
S
O2
0
500
1000
1500
2000
2500
3000
3500
Time (sec)

(b)

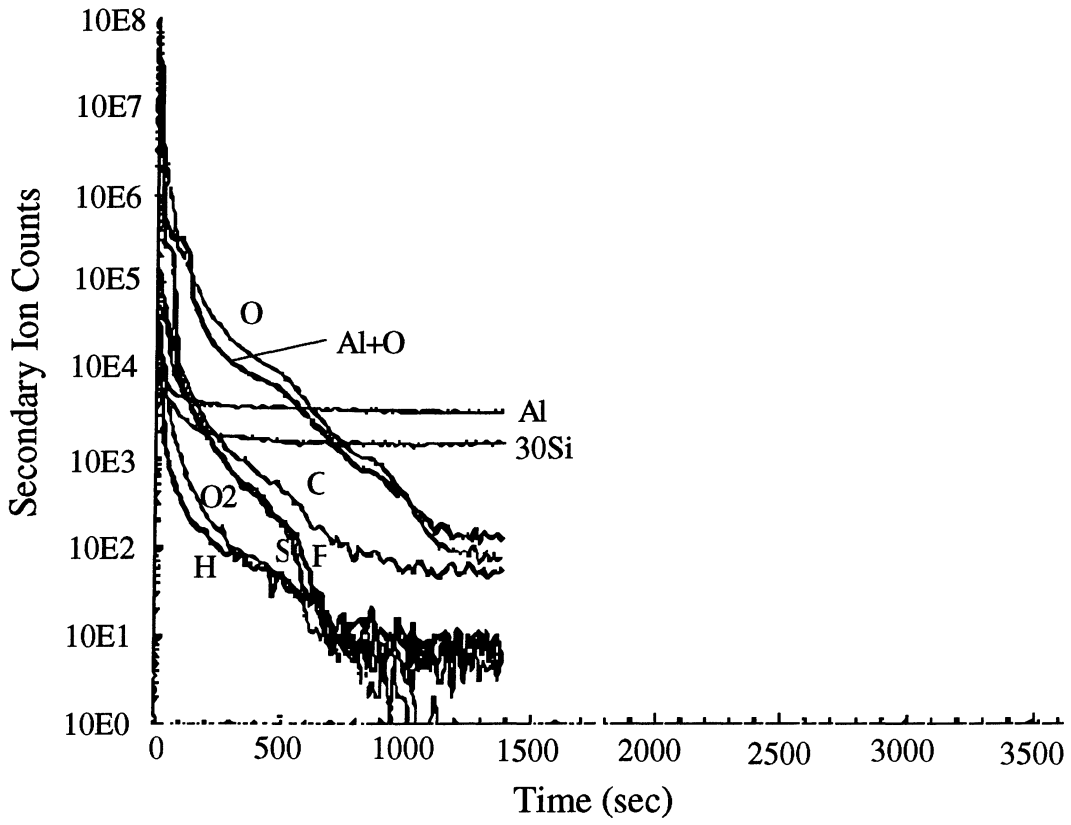

(c)

Fig. 15 - SIMS Depth Profiles

(a) Dark Spot on the Wear Scar, (b) Shiny Spot on the Wear Scar, (c) Virgin Surface

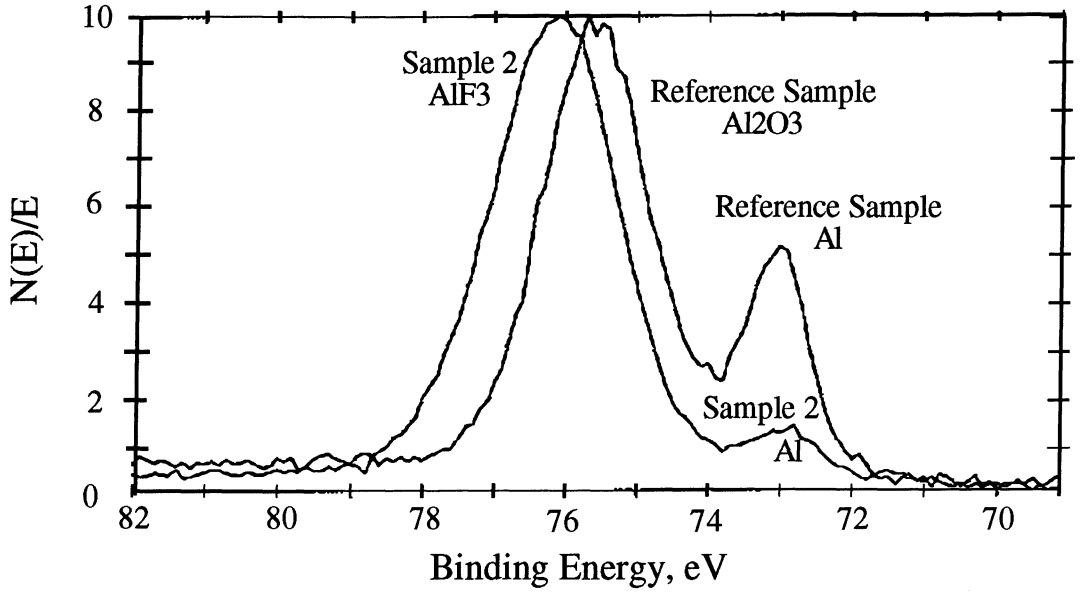

Fig. 16 - XPS Study on a Worn Under R134a (Sample 2) and Virgin Surfaces (Reference Sample)

5. SUMMARY

Friction and wear tests of various aluminum alloys, aluminum composites and some surface treated aluminum alloys lubricated with different L/R mixtures were conducted using the HPT. These materials were slid against 1018 carburized steel pins. The L/R mixtures tested included mineral and alkylbenzene lubricants with R22, R407C and R410A, an ester lubricant with both R407C and R410A, and PAGs and esters with R134a. Most of the friction and wear data obtained were for 356-T61 and 390-T6 aluminum alloys. The effects of the viscosity of the L/R mixture and the initial surface roughness of the aluminum specimens were also evaluated. Finally, the effect of the environmental pressure of R134a refrigerant on the surface fatigue of 356-T61 alloys was analyzed. The results can be summarized as follows:

- The 2024-T351 and 6061-T61 alloys have approximately two orders of magnitude higher wear than the other materials tested. The friction coefficient of these alloys is also significantly higher and the contact resistance is lower than that of other alloys.
- In general, the amount of wear decreases as the amount of silicon content increases. This trend, however, is complicated by the presence of other alloying elements and the different heat treatment processes.
- The addition of bismuth and higher amount of copper reduces wear for alloys of otherwise similar composition and heat treatment.
- The lowest wear is obtained with the 390DC-T6 alloy. The HV4-T61 alloy also gives very good wear resistance.
- Conventional anodizing (356CM-AN-Fig. 6) does not improve the wear resistance of the 356 aluminum alloy under concentrated contacts. The hard layer cracks under the high contact stress causing an increase in wear.
- The Ester/R134a mixtures consistently provided better protection of the aluminum disc specimens compared to the PAG/R134a mixtures, even though the viscosity of the Ester/R134a mixture is lower than that of the PAG/R134a mixture.
- Hard anodizing and SiC particle reinforcement provide very good wear resistance. However, they cause increased wear on the counterface due to the rough hard surfaces generated by hard anodizing processes and the hard SiC particles on the surface of a SiC-Al composite.

- With the exception of condition F, the wear depths on 390PM-T61 alloy were consistently smaller than those on 356CM-T61 alloy.

- The capped PAG (PAG 2) seems to be a better lubricant for 356CM-T61 alloy than the uncapped lubricant (PAG 1). However, for the 390PM-T61 alloy, the lubricity of the PAG's is about the same.

- When Ester 1 lubricant is used, the wear on the discs of both alloys is about the same in R134a, R407C, R410A and air environments.

- The R407C and R410A used with alkylbenzene lubricant provide similar (with 390PM-T61) or slightly better (with 356CM-T61) wear resistance when compared to R22. The lower wear obtained with the 356CM-T61 alloy is probably due to the higher viscosity of alkylbenzene/R407C or R410A mixtures compared to the alkylbenzene/R22 mixture. However, the relative wear differences between these mixtures are small, therefore, more tests need to be conducted to examine their lubricity difference, if any exists.

- The mineral/R22 mixture produces less wear (with 356CM-T61) than the other mixtures, even though the viscosity of the mineral/R22 mixture is smaller than that of the other mixtures. However, with the 390PM-T61, it is the mineral/R407C mixture which provides slightly better wear resistance compared to the other mixtures.

- The R134a refrigerant does not always behave as an inert environment. Under the conditions of this study, a chemical reaction between the freshly exposed aluminum and R134a occurred. The reaction product was identified as AlF_3.

- R134a and other HFC's at sufficiently high partial pressures increase the brittleness of aluminum alloys. Corrosion cracking and/or hydrogen embrittlement are viewed as possible mechanisms. The formation of AlF_3 on freshly exposed aluminum surfaces may be another reason for the enhanced brittleness. However, the actual causes and mechanisms for the surface fatigue on the 356 alloys are not clear at this time.

6. FUTURE RESEARCH

The seizure resistance of aluminum alloys and tribological behavior under starved lubrication condition are the next areas of emphasis for this project.

7. REFERENCES

1. **Davis J.R.**, *ASM Specialty Handbook, Aluminum and Aluminum Alloys*, ASM International, Materials Park, OH, 1993.
2 **Somi Reddy, A., Pramila Bai, B. N., Murthy, K. S.S., and Biswas, S. K.**, Wear and Seizure of Binary Al-Si Alloys, *Wear*, 171 (1994) 115-127.
3 **Sarkar, A. D. and Clarke, J.**, Friction and Wear of Aluminum-Silicon alloys, *Wear*, 61 (19800 157-167.
4 **Sarkar, A. D.**, Wear of Aluminum-Silicon Alloys, *Wear*, 31 (1975) 331-343.
5 **Torabian, H., Pathak, J. P. and Tiwari, S. N.**, Wear Characteristics of Al-Si Alloys, *Wear*, 171 (1994) 49-58.
6 **Hanna, A. H. and Shehata**, F., Friction and Wear of Al-Si Alloys, *Lubrication Engineering*, 49, (1992) 473-476.
7 **Konishi, T., Klaus, E. E. and Duda, J. L.**, Wear Characteristics of Aluminum-Silicon Alloy Under Lubricated Sliding Conditions, STLE Preprint No. 95-MP-5E-1, 50th Annual Meeting of STLE, Chicago, Illinois, May 14-19, 1995.
8 **Davis, F. A. and Eyre, T. S.**, The Effect of silicon Content and Morphology on the Wear of Aluminum-Silicon Alloys Under Dry and Lubricated Sliding Conditions, *Tribology International* 27 (1994), 3, 171-181.
9 **Barber, G. C., Matthews, J. J. and Jafry, S.**, Wear and Scuff Resistance of Aluminum 390, *Lubrication Engineering*, 47 (1991) 423-430.
10 **Ferrante, J. and Brainard W. A.**, Wear of Aluminum and Hypoeutectic Aluminum-Silicon Alloys in Boundary Lubricated Pin-on-Disk Sliding, NASA Technical Paper 1442, (1979).
11 **Tseregounis, S. I.**, Wear and Galling of 356-T6 Aluminum-on-Steel in Low Amplitude Reciprocating Sliding in the Presence of Synthetic Lubricants in HFC-134a Atmosphere, STLE Preprint No. 95-AM-1C-1, STLE 50th Annual Meeting, Chicago, IL, May 14-19, 1995.
12 **Okabayashi, K. and Kawamoto, M.**, Influences of Silicon Content and Grain Size of Primary Silicon Crystals on the Wear of High Silicon Aluminum Alloys, *Bulletin of University of Osaka Prefecture*, 19 (1968) 199-216.
13 **Pramila Bai, B. N, and Biswas, S. K.**, Scanning Electron Microscopy Study of Worn Al-Si Alloy Surfaces, *Wear*, 87 (1983) 237-249.
14 **Jasim, M. K. and Dwarakadasa, E. S.**, Wear in Al-Si Alloys Under Dry Sliding Conditions, *Wear*, 119 (1987) 119-130.
15 **Antoniou R. and Subramanian, C.**, Wear Mechanism Map for Aluminum Alloys, *Scripta Metallurgica*, 22 (1988) 809-814.
16 **Subramanian C.**, Some Considerations Towards the Design of a Wear Resistant Aluminum Alloy, *Wear*, 155 (1992) 193-205.
17 **Razavizadeh, K. and Eyre, T. S.**, Oxidative Wear of Aluminum Alloys, Wear 79 (1982) 325-333.
18 **Sharma, A. and Rajan, T. V.**, Scanning Electron Microscopic Studies of Worn-out Leaded Aluminum-Silicon Alloy Surfaces, *Wear* 174 (1994) 217-228.
19 **Pramila Bai, B. N. and Biswas, S. K.**, Mechanism of Wear in Dry Sliding of a Hypoeutectic Aluminum Alloy, *Lubrication Engineering* 43 (1987) 57-61.
20 **Rohatgi, P. K. and Pai, B. C.**, Effect of Microstructure and Mechanical Properties on the Seizure Resistance of Cast Aluminum Alloys, *Wear* 28 (1974) 353-367.
21 **Sargent, Jr. L. B., Milz, W. C. and Atkinson, R. E.**, The Effect of Aluminum Transfer Upon the Friction Between Aluminum Alloys and Steel, *Lubrication Engineering* 39 (1983) 706-711.
22 **Ni, X. and Cheng, H. S.**, Seizure Resistance of Aluminum-Lead-Silicon Connecting Rod Bearings and Nodular Cast Iron Shafts, STLE Preprint No. 95-AM-5B-2.
23 **Ni, X. and Cheng, H. S.**, Seizure Failure of Copper-Lead with Overlay and Aluminum-Tin Connecting Rod Bearings, STLE Preprint No. 95-AM-58-3, STLE 50th Annual Meeting, Chicago, IL, May 14-19, 1995.
24 **Beesly, C., and Eyre, T. S.**, Friction and Wear of Aluminum Alloys Containing Copper and Zinc, *Tribology International* 9 (1976) 63-69.
25 **Pathak, J. P., Tiwari, S. N., and Malhotra, S. L.**, On the Wear Characteristics of Leaded Aluminum Bearing Alloys, *Wear* 112 (1986) pp. 341-353
26 **Tiwari, S. N., Pathak, J. P., and Malhotra, S. L.**, Seizure Resistance of Leaded Aluminum Bearing Alloys, *Materials Science and Technology* 1 (1985) 1040-1045.
27 **Rohatgi, P. K., Liu, Y., and Ray, S.**, Friction and Wear of Metal-Matrix Composites, in ASM Handbook Vol. 18, Friction, Lubrication and Wear Technology (1992).
28 **Lee, C. S., Kim, Y. H., Han, K. S., and Lim, T.**, Wear Behaviour of Aluminum Matrix Composite Materials, *Journal of Material Science* 27 (1992), 2, 793-800.

30 **Kawamura, M., and Fujita, K.**, Antiwear Property of Lubricant Additives for High Silicon Aluminum Alloy Under Boundary Lubricating Conditions, *Wear* 89 (1983) 99-105.
31 **Montgomery, R. S.**, Chemical Effects on Wear in The Lubrication of Aluminum, *Wear* 8 (1965) 289-302.
32 **Montgomery, R. S.**, The Effect of Alcohols and Ethers on the Wear Behavior of Aluminum, *Wear* 8 (1965) 466-473.
33 **Montgomery, R. S. and Garret, H. L.**, An Electron-Microscopic Study of Aluminum Wear Particles Formed During Sliding in the Presence of Polyglycols, *Wear* 10 (1967) 310-312.
34 **Montgomery, R. S.**, The Lubrication of Aluminum by Phtalic Acid Esters, *Wear* 9 (1966) 297-299.
35 **Laemmle, J. T. and Bohaychick, J.**, Novel Substituted Manolic Diesters: Effectiveness of Bidentate Bonding of Additives on Aluminum Workpiece Surfaces, *Lubrication Engineering* 43 (1986), 9, 717-722.
36 **Hotten, B. W.**, Bidentate Organic Oxygen Compounds as Boundary Lubricants for Aluminum, *Lubrication Engineering* 30 (1974), 8, 398-403.
37 **St. Pierre, L. E., Owns, R. S., and Klint, R. V.**, Chemical Effects in the Boundary Lubrication of Aluminum, *Wear* 9 (1966) 160-168.
38 **Sargent, L. B.**, The Influence of Aluminum Oxides on the Transfer of Some Aluminum Alloys to Steel in Sliding Contact, *Lubrication Engineering* 38 (1982) 10, 615-621.
39 **Davis, B., Sheiretov, T., and Cusano, C.**, Tribological Evaluation of Contacts Lubricated by Oil-Refrigerant Mixtures, *1992 International Compressor Engineering Conference at Purdue*, Purdue University, W. Lafayette, IN, 477-487, July 14-17, 1992.
40 **Sheiretov, T. K., VanGlabbeek, W. H., and Cusano, C.**, The Effect of Dissolved Water on the Tribological Properties of Polyalkylene Glycol and Polyolester Lubricants, STLE Preprint No. 95-TC-2C-1, STLE/ASME Tribology Conference in Kissimmee, Florida, October 8-11, 1995.
41 **Komatzuzaki, S., Homma, Y., Itoh, Y., Kawashima, K., and Iizuka, T.**, Polyol Esters as HFC-134a Compressor Lubricants, *Lubrication Engineering* 50 (1994) 801-807.
42 **Holm, R.**, Electric Contacts Theory and Applications, Springer-Verlag, New York, 1967.